Alma Mater Studiorum - Università di Bologna

SCUOLA DI SCIENZE

Dipartimento di Chimica Industriale "Toso Montanari"

Corso di Laurea Magistrale in

Chimica Industriale

Classe LM-71 - Scienze e Tecnologie della Chimica Industriale

Bionanocomposites based on PLLA, PCL and Montmorillonite: synthesis, characterization and crystallization

Tesi di laurea sperimentale

CANDIDATO

Giacomo Bettini

RELATORE

Chiar.mo Prof. Daniele Caretti

CORRELATORE

Prof. Alejandro J. Müller

Dott. Matteo Rizzuto

Sessione III

Anno Accademico 2014-2015

ABSTRACT

Poly(lactide) (PLA) seems to be the best candidate to replace conventional petroleum-based polymers, since it is bio-based, biocompatible and biodegradable. However, commercial PLA materials typically have low crystallization rate resulting in long processing time and low production efficiency.

In this work the effects of two different type of clay based nanofillers (MMT30B and MMT30B-g-P(LA-co-CL)) on the crystallization rate of neat PLA and 80/20 PLA/PCL blend were investigated.

MMT30B-g-P(LA-co-CL) was synthetized by the *in situ* grafting reaction of the random copolymer P(LA-ran-CL) on montmorillonite (MMT30B). The synthesis was carried in xylene at 140°C, upon the results of a solvent and temperature screening. The composition of the grafted copolymers on the organoclay were evaluated by ^{1}H-NMR whereas the amount of clay in the nanofiller was evaluated by ATR–IR and TGA.

Solvent casted films were obtained by solution mixing of MMT30B-g-P(LA-co-CL) at 5% (w/w) with neat PLA and PLA/PCL blend, comparing the properties with the corresponding PLA and PLA/PCL blends with and without a 5% of (w/w) unmodified clay.

SEM micrographs on PLA/MMT30B and PLA/MMT30B-g-P(LA-co-CL) shows that MMT30B it is aggregated into larger particles compared to MMT30B-g-P(LLA-co-CL). This behavior it's correlated to the better exfoliation of MMT30B-g-P(LA-co-CL) clay layers upon the intercalation of the copolymer grafted chains. SEM micrographs on PLA/PCL based blends exhibit the typical *sea-island* morphology, characteristic of immiscible blends. PLA is the matrix while PCL is finely dispersed in droplets. MMT30B does not reduce PCL droplets size. On the contrary, upon the addition of MMT30B-g-P(LA-co-CL), PCL droplets are significantly reduced. This means that, thanks to the grafted copolymers chains, MMT30B-g-P(LA-co-CL) can migrate to the PLA-PCL interface, acting as a compatibilizer.

Non-isothermal DSC cooling scans show a fractionated crystallization of the PCL phase in PLA/PCL/MMT30B-g-P(LA-co-CL), confirming the compatibilizer effect of MMT30B-g-P(LA-co-CL). At the same time, being more dipersed than MMT30B, MMT30B-g-P(LA-co-CL), can better nucleate the PLA phase, both in neat PLA and PLA/PCL blend, promoting the crystallization during the heating scans. On the contrary in isothermal condition, both the nanofillers increase the crystallization rate of PLA phase in neat PLA at the same way, while in PLA/PCL blends the effect is covered by the nucleating effect of PCL.

Keywords: grafted random copolymers, montmorillonite, overall crystallization rate, isothermal crystallization rate, poly(L-lactide).

ABBREVIATIONS USED IN THE THESIS

LA = racemic lactide

LLA = L-lactide isomer

CL = ε-caprolactone

PLA = poly(lactide)

PLLA = poly(L-lactide)

PDLA = poly(D-lactide)

PCL = poly (ε-caprolactone)

MMT30B = montmorillonite 30B

MMT30B-g-P(LLA-co-CL) = Random copolymer poly(L-lactide-*co*-ε-caprolactone) grafted on montmorillonite 30B

SEM = Scanning Electron Microscopy

DSC = Differential Scanning Calorimetry

TGA = Thermal Gravimetric Analysis

ATR-IR= Attenuated total reflection infrared spectroscopy

^{1}H-NMR = Hydrogen-1 Nuclear Magnetic Resonance

Tm = melting temperature

Tm^{0} = equilibrium melting temperature

Tc = crystallization temperature

ΔT = supercooling (Tm^{0}-Tc)

1 INTRODUCTION

In the recent years polymers have reached more and more attentions because of their quality like lightweight, strenght, low cost, ease of modification and their chemical inertness even if they present environmental problems especially thinking about the disposal at end of life.
For these reasons, in the last years with the increase of public attention on environmental problems, the research of biodegradable polymers has collected considerable interest [1].
This develop has brought to a reconsideration about polymer both natural and synthetic with a special attention to alyphatic polyesters which has two important characteristics: biodegrability and biocompatibility.
Biopolymers are classified according to the "European Bioplastics Association" as biodegradable polymers approved according to EN 13432 that come from renewable sources. Moreover, it's important to underline that polymers from renewable sources can be either biodegradable or not biodegradable [2].
Biodegradable polymers are divided in three categories related to the source and the production process:

- Polymers from biomass like lipids, proteins and polysaccharides;
- Polymers synthetized from monomers arising from both biomass and oil;
- Polymers produced by microorganisms and genetically modified bacteria [3].

One of the most interesting and most studied biopolymer is polylactide (PLA) as demonstrated by the multitude of publications, rewiev and book on it [3], [4].
These studies report that PLA is biodegradable and biocompatible allowing its use in medicine with living tissue.
One of the first things, that we have to consider talking about PLA, is that the structure and morphology of a semi-crystalline polymer are foundamental to be understood to evaluate their thermodynamic, physical and mechanical properties.
Moreover, understanding how crystallization rate and crystallization mechanism occur is the key to understand the behavior of PLA [5], [6].
A new strategy studied to overcome the slow crystallization rate is linked to the use of nanocomposites. One of the solution proposed is to use organo-modified clay to increase the crystallization rate of PLA [7].

To obtain appreciable increment in crystallization rate it is foundamental that the organo-clay reaches an high degree of dispersivity in the generally hydrophobic polymer matrix without the presence of aggregation process. Moreover a good interfacial adhesion is needed.
Two approaches to reach the terms above mentioned were proposed and both consist in a surface modification of the clay:

- the first consist in the insertion of a hydrophobic, organic sostituent on montmorillonite;
- the second one results in the grafting of polymer chains on the organic sostituent of the clay using two approaches: "*grafting from*" and "*grafting to*".

Talking more about the second pathway, the "*grafting from*" technique was preferred because, as reported in previous studies, [8] it allows to reach a higher degree of exfoliation and a higher grafting density of polymer on the clay than the other technique.
In this study, to achieve the grafting of the copolymer on the surface of the clay, we worked using a chain polymerization called surface-initiated ring-opening polymerization (SI-ROP).
The initiator for this polymerization were the hydroxyl groups of the quaternary ammonium salt present as substituent on montmorillonite. The reaction was catalyzed by tin (II) 2-ethylhexanoate ($Sn(Oct)_2$) and the monomers used were ε-caprolatone (CL) and L-lactide (LLA).

1.1 Polyester

One of the most important group of biodegradale and biocompatible polymers are linear aliphatic polyester.
It's important to underline that not all the polyesters are biodegradable, but only the ones containing methylene segments between the ester groups will degrade in reasonable time. Degradation of polyesters can be made by enzymes or by biological conditions or by a combined action of both the processes. The mechanism of degradation is characterized by a hydrolytical cleavage of the ester bond.
In this work are threated polyesters derived from ε-caprolactone and lactide that in the last years had joined great interest because, in addition to be biodegradable, there are also biocompatible allowing to be used in devices for controlled drug delivery and in biomedical applications.

However there are some restrictions about using these polyesters due to their poor mechanical and thermal properties, but researcher are trying to solve these problems with different strategies like mixing them with different polymers in blends or performing copolymerization reactions.

1.1.1 Poly(ε-caprolactone), PCL

PCL is one of the most studied polyester because of its characteristics.

First of all, even if the raw material used for his preparations come from oil or more generally from non-renewable sources, the polymer is completely biodegradable because the ester bond is easily hydrolized [9].

PCL is a semi-crystalline polymer with glass transition temperature at -60°C and melting point at 60°C which slightly change as a function of its crystallinity degree [10].

The amorphous phase of this polymer presents an unusual behavior with respect other aliphatic polyesters; in fact this phase is always rubber-like making PCL permeable to a lot of active principles. This characteristic and its biocompatibility allow its use in devices for the controlled release of drugs and in biomedical application.

PCL displays the rare property of being miscible with many other polymers like poly(vinyl chloride), poly(styrene-co-acrylonitrile) and polycarbonates creating the conditions to form copolymers with very different properties from the starting monomers or to form compatible blends, while, if mixed with the majority of aliphatic polyesters, it forms immiscible blends [10].

The most common and studied way of synthesis for PCL in the last years is the polymerization starting from ε-caprolactone monomer by Ring-Opening Polymerization (ROP). This process use alcohols with one, two or multi-functional hydroxyl groups as initiator in the presence of a coordination complex (usually containing Sn, Zn, Al), typically obtained from compounds such as $Sn(Oct)_2$.

Polymerization starts from nucleophile species such as alcohol, both in the presence or absence of catalysts. In presence of organometallic species as catalyst the reaction proceeds forming alkoxides which are responsible for the polymerization of the monomers according to a mechanism of coordination-insertion as shown in Figure 1.1 [10].

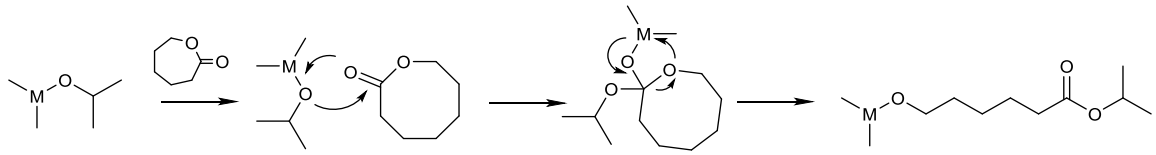

Figure 1.1 Mechanism of the initiation step for coordination–insertion ROP, adapted from Khanna et al.[11] and Stridsberg et al. [12]

1.1.2 Poly(lactic acid), PLA

Lactic acid used for the polymerization to poly(lactic acid) is industrially prepared by bacterial fermentation process of carbohydrate starch. This process allow to obtain percentage of the L(-) isomer near to the 99.5%.

Polymers based on poly(lactic acid) are mainly used food, pharmaceutical, textile, leather and chemical industries [13].

Polycondensation reaction to directly obtain the polyester is enabled by the presence of both a hydroxyl and a carboxyl group in lactic acid. However, the molecular weight obtained is not high enough for industrial application even if organic solvents are used for azeotropic distillation of condensation water and the polymerization time is very long [14].

To obtain high-molecular-weight poly(lactic acid) the most common process contemplate the ring-opening polymerization of lactide.

Lactide, a cyclic lactic acid dimer, is formed in the direct condensation when water is removed by evaporation or when L-lactic acid, D-lactic acid or mixtures thereof are polymerized to corresponding low-molecular-weight poly(lactic acid) oligomer and then, subsequently depolymerized, the oligomer 'back-biting' reaction forms lactide.

Three isomers of lactide are possible: L-lactide, D-lactide, and meso-lactide.

In the second step, purified L-lactide, D-lactide or meso-lactide monomer is converted into the corresponding high-molecular weight polyester by catalytic ring-opening polymerization carried out most commonly by a stannous octoate catalyst.

Stannous alkoxide, a reaction product between stannous octoate and alcohol, is proposed as the substance initiating the polymerization through coordinative insertion of lactide [13].

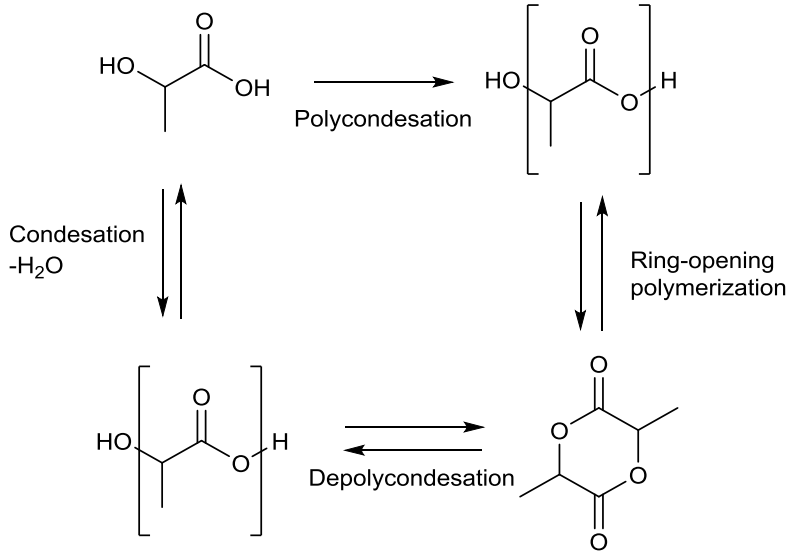

Figure 1.2 PLA production via lactic acid and lactide.

Properties of this polymer, as indeed those of other one, depend on the degree of crystallinity, molecular weight and stereochemistry. The physical properties of PLA are related to the enantiomeric purity of the lactic acid. PLA can be produced in a totally amorphous phase or with up to 40% crystalline. If the amount of L-lactic acid is over 93% we have a semicrystalline polymer; if the amount is between 50 and 93% it is completely amorphous. Changing the composition in terms of L-lactic acid inside a PLA macromolecule it is possible to pass from elastic behavior (amorphous PLA) to the rigid one (semicrystalline PLA), with the possibility to change mechanical properties according to specific requirement.

Moreover the degree of crystallinity influences the tendency of this polymer to degrade by hydrolisis process. It has been demonstrated that, increasing the amount of crystallinity in the polymer, there is a raise in terms of water permeability and in consequence of this a high cristallinity PLA requires several months to degrade, while the amorphous form degrades in few weeks.

The melting point and the glass transition temperature (Tg) of PLA are strongly dependent on the molar mass and optical purity of the polymer, among other factors. The thermal history of the polymer affects these values as well.

The main application areas of PLA are packaging and biomedical materials, where, in particular, the Tg and the Tm largely determine the suitability of the polymer for the application.

The thermal transitions (Tg, crystallization temperature (Tc), and Tm) and the related enthalpies of PLA are often determined using differential scanning calorimetry (DSC).

The Tg of high-molecular-weight PLA is nearby 60°C, while Tm is typically in the range between 170 and 180°C because of the presence of the different enantiomers and other impurities that lead to imperfect crystals [15].

In Figure 1.3 are reported the three different structures in which PLA could exist: PLLA, PDLA and PDLLA. PLLA and PDLA are the stereoregular (isotactic) semi-crystalline forms, while PDLLA is amorphous because it is an atactic polymer constituted by units of both D-lactic acid and L-lactic acid.

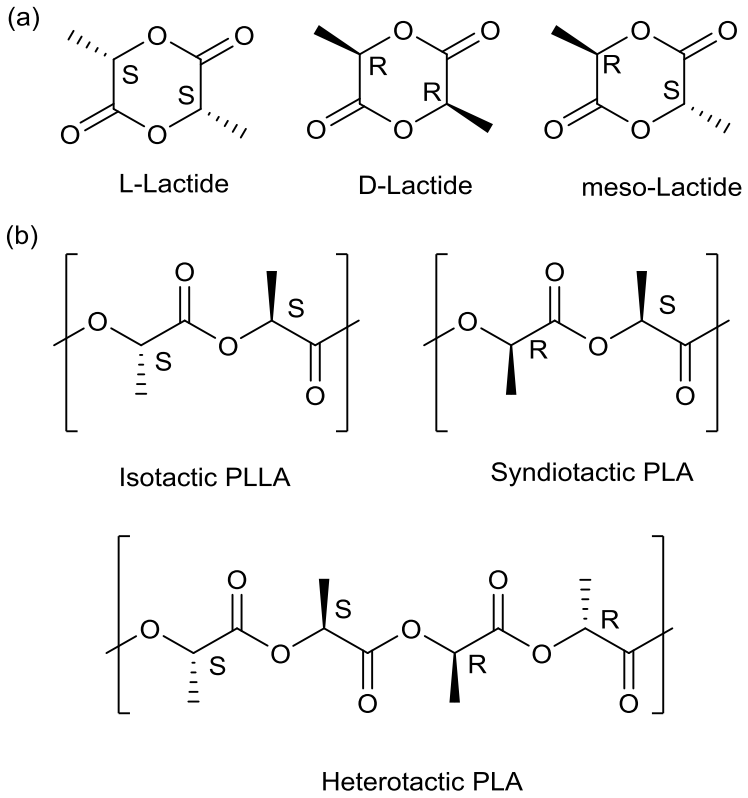

Figure 1.3 Stereochemistry of a) lactid acid and b) of the different poly(lactic acid).

The rate of crystallization is comparable to the one of poly(ethylene terephthalate) (PET), resulting in a quite slow process [2].

Moreover PLA is a brittle polymer and this aspect limits a lot its use.

A pathway to reach a solution to these problems is to blend of PLA with different polymers. Applying this technique it is possible to modulate the properties of the different mixtures of polymers depending on the use that them are required for, obtaining characteristics very different from the one of the homopolymers.

For example a typical blend studied is composed by PLA and PCL in which, the final characteristics of the blend is modulated as a function of the ratio of the two polymers.

1.2 Montmorillonite

Nanoclays used as fillers have gained great popularity due to their attractive platelet-like nanostructures. The unique structure and property of nanoclay fillers have resulted in the manufacture of numerous polymer/clay nanocomposites with the aim of alleviate the worsened mechanical and thermal properties of biopolymers.

Typical montmorrillonite (MMT) clays are regarded as one of the most effective nanofillers used in polymer/clay nanocomposites due to their low material cost and easy intercalation and modification [16].

MMT nanoclays are also known as 2:1 phyllosilicates and possess a layer of octahedral alumina and two linked tetrahedral silicate layers, illustrated in Figure 1.4.

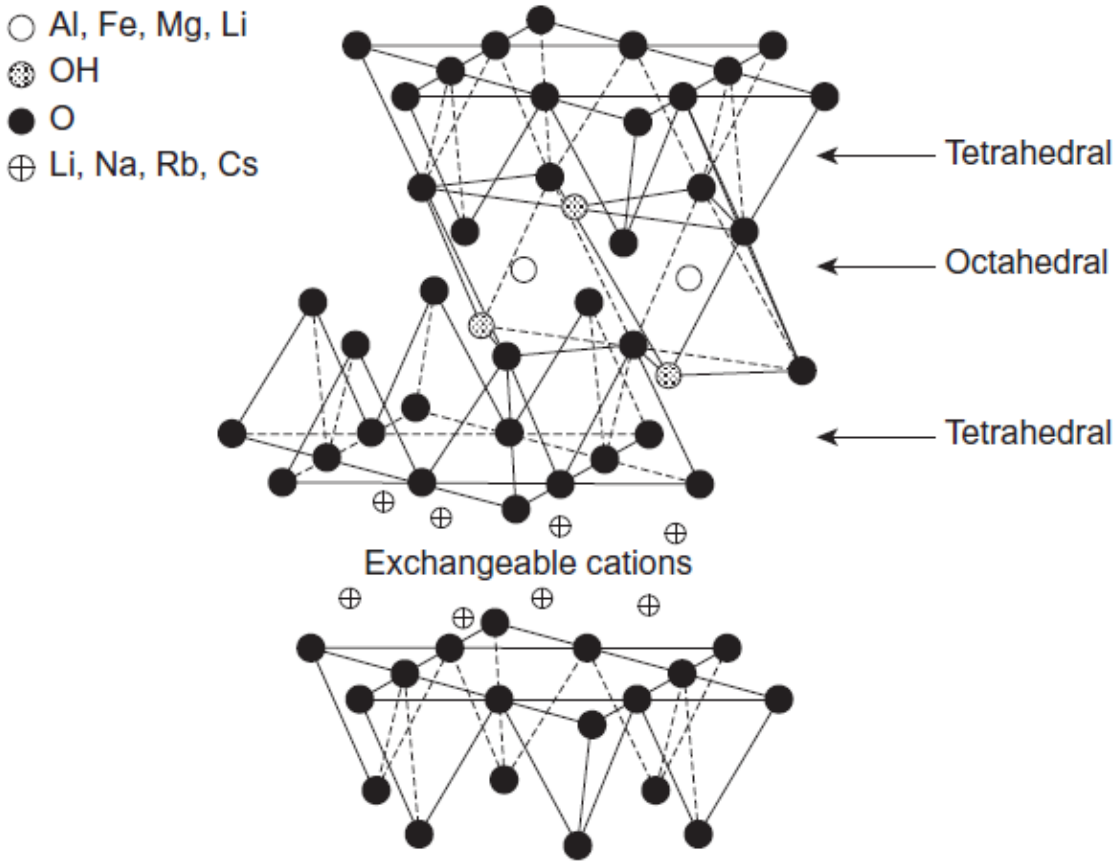

Figure 1.4 Sheet- like montmorillonite structure [17].

A hexagonal symmetry is formed from one silicium atom and four joint oxygen atoms on the outer tetrahedral layer. Meanwhile, each aluminum atom is bonded with six oxygen atoms in the shape of an octahedron (i.e., a polyhedron with eight faces) on the octahedral layer with

each phyllosilicate layer being linked by Van der Waals interactions through the interlayer galleries.

The aluminum sheet can be easily replaced with a cation. Al^{3+} cation may be substituted by Mg^{2+} or Fe^{2+} to produce a negative charge on the layer that must be balanced by alkali cations such as Na^{+}, Rb^{+}, Cs^{+}, or Li^{+}.

A single phyllosilicate layer has a typical thickness of 1 nm, whereas the thickness of its particle is in the range between 30 nm and few microns [18].

MMT nanoclays are of wide use due to their easy modification with organic cations on the interlayer gallery.

Several processing parameters that can influence the interactions between nanoclay particles and polymer molecules are known:

- clay dispersion;
- clay modification;
- compatibility between nanoclays and polymer matrices;
- catalyst of curing agents for thermosetting materials.

Consequently, to understand the mechanism of natural clay modification is essential.

The surfaces of organoclays can be tailored to alter their chemical properties and compatibility with polymer matrices.

The cation-exchange method is essential for surface modification by changing the cation ion with an organic surfactant, and to modify organophobicity into organophilicity. In the past two decades, many researchers discovered that the modification of interlayer and surface of organoclays could be used to optimize the material performance and properties of polymer/clay nanocomposites [18].

Montmorillonite30B is prepared exchanging Na cation with (methyl tallow bis-2-hydroxyethyl) quaternary ammonium salt.

As mentioned before this step is foundamental to improve the organophilicity of the clay and to increase the space between the layers. Moreover the hydroxyl groups present on this salt are used to start the in-situ polymerization of the copolymer on the clay.

However, the properties of polymer/clay bionanocomposites are also known to be affected by the compatibility and reactivity of biopolymers and nanoclays, their manufacturing methods and processing parameters [19].

In particular the morphological structures of polymer/clay bionanocomposites rely on the processing conditions and methodology of material synthesis. Alexander and Dubois

reviewed the structures of polymer/clay nanocomposites and indicated three possible structure: microcomposites, intercalated, and exfoliated as demonstrated in Figure 1.5 [17]:

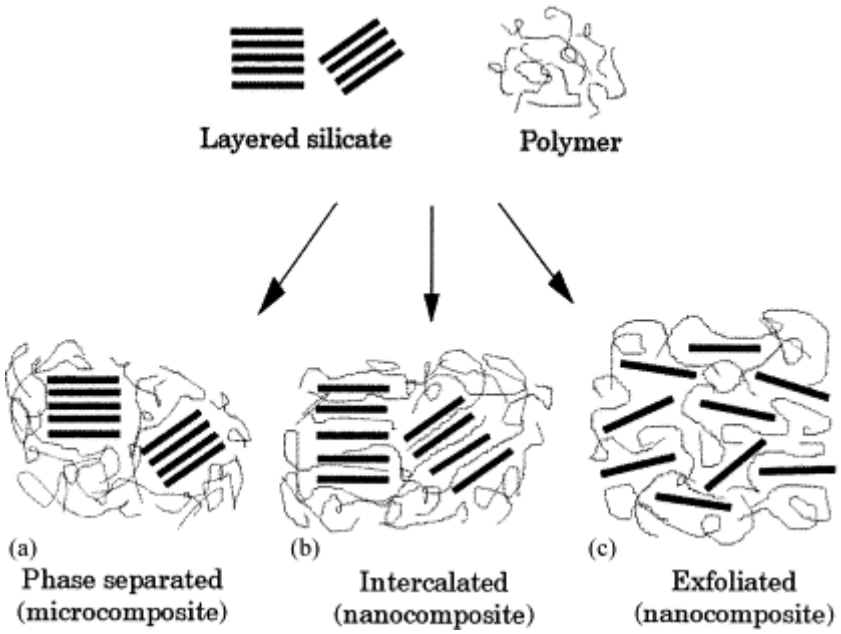

Figure 1.5 Different morphological structure of clay/polymer systems [17]**.**

When clay aggregates are separated from polymer matrices without the change of clay basal spacing, this results in microcomposites due to the micron-sized clay aggregates. As polymer molecules are inserted into clay particles to broaden clay interlayer areas, intercalated structures occur. When polymer molecules are diffused into clay gallery with sufficient interlayer spacing, it leads to exfoliated structures with superior properties of nanocomposites. In the in-situ polymerization process, clay nanofillers are directly mixed with monomers. Then the monomers diffuse into clay interlayers to produce clay intercalation structures. The final polymerization process can be achieved either by heat, radiation, or by the diffusion of initiators or catalysts [20].

The processing conditions are controlled by temperature, mixing speed, mixing time, and shear stress generated from the rotor or blade of a mixer [17].

1.3 Grafting to and grafting from techniques

One way to improve the adhesion between polymer matrices and the nanoclay is to modify clay's surface grafting polymer chains on it.

Two different approaches are mainly studied and used to do this modification they are called "grafting from" and "grafting to" .

In "grafting from" approach, the monomers are directly polymerized on the clay surface. With this technique is possible to obtain a good degree of exfoliation and a high grafting density.
"Grafting to" consists in a pre-formed polymer subsequently bound to the surface of the organoclay. It could be achieved in two different ways:

- through a covalent bond by reacting one chain end of the polymer with functionalities on the ammonium salt presents on the organoclay surface;
- through non-covalently interactions.

One of the advantages in the use of the "grafting to" technique is the high molecular weight polymer that can be used, but, using these polymers, there are limitations in the process of intercalation and exfoliation of the organoclay .
In this study, "*the grafting from*" was preferred, since a better organoclay exfoliation is obtained. There are different ways to obtain the grafting on the organoclay surface, but, considering that our monomers of interest are lactide and ε-caprolactone, we chose to perform a chain polymerization named Surface-Initiated Ring-Opening Polymerization (SI-ROP).
The most accredited (SI-ROP) mechanism is coordination-insertion. This mechanism is based on metal alkoxides having a covalent bond between oxygen and metal, with a weak Lewis acid behavior.
The lactide and ε-caprolactone behave as a ligand that coordinates the metal atom with the oxygen bound to the carbonyl.

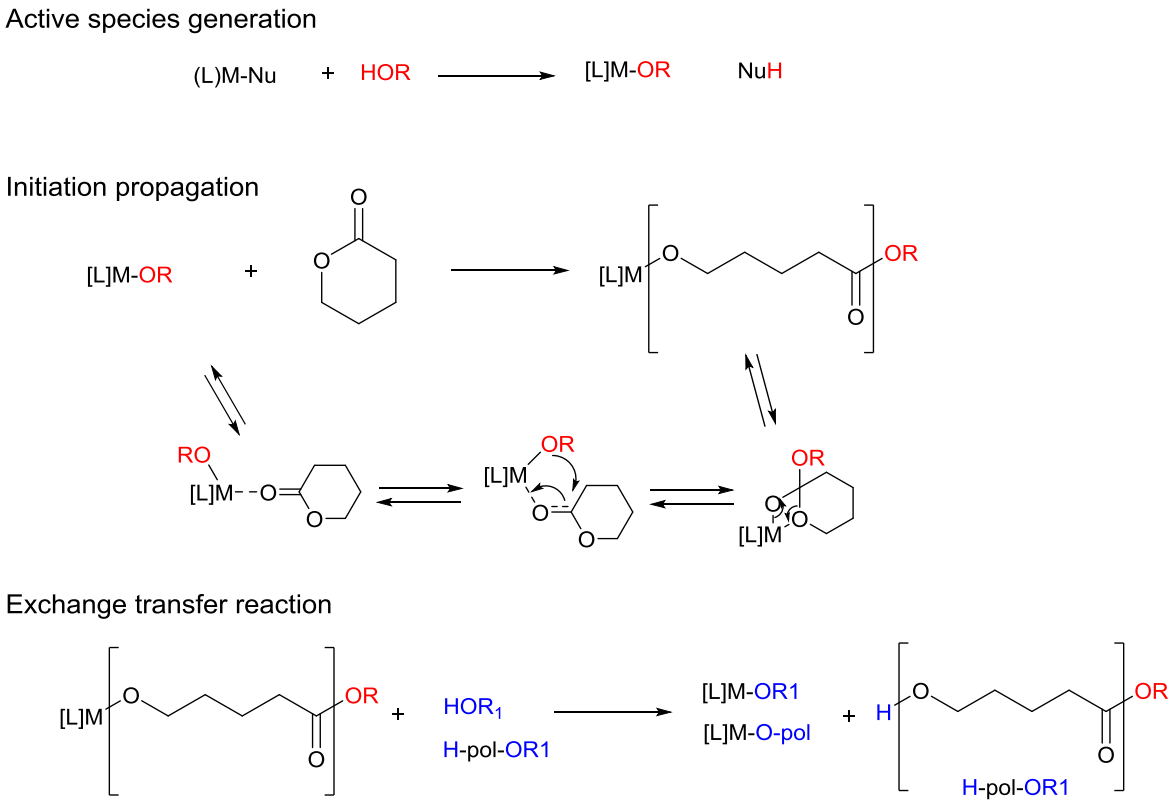

Figure 1.5 Proposed reaction pathway for the ROP of a cyclic ester by the coordination-insertion mechanism [21].

This mechanism improves both the electrophilicity coordination of the carbonyl group and the nucleophilicity of the alkoxide group. This allows the insertion of the lactide and ε-caprolactone in the metal-oxygen bond [21].

Alkoxides of magnesium, aluminium, tin, zirconium and zinc are typical initiators for this mechanism. Tin(II)octoate ($Sn(Oct)_2$) is the most used compound due to its solubility, high catalytic activity and its capacity to promote the formation of a high molecular weight polymers with low level of racemization (<1%) and the peculiarity of low toxicity level; in fact US Food and Drug Administration (FDA) allows its use.

In our work we used the hydroxyl groups of the ammonium salt presents on the organoclay surface as initiator, tin(II)-2-ethylhexanoate ($Sn(Oct)_2$) as catalyst and finally ε-caprolatone (CL) and L-lactide (LLA) as monomers.

1.4 PLA/PCL blends

Blending is a relatively simple and rapid approach to evaluate the interactions between two or more different polymers and to create a new material with physical properties different from the starting ones.

Both fusion and solution processes could be used to prepare blends.

Binary blends can be classified by the conformation of the polymers in:

- amorphous/amorphous;
- semi-crystalline/amorphous;
- semi-crystalline/semi-crystalline.

Blends containing a semi-crystalline and an amorphous polymers are the most used because they presents a good balance of mechanical properties such as impact resistance, toughness and ductility.

Blends can be also classified in other three categories:

- miscible blends;
- semi-miscible blends;
- immiscible blends.

Immiscible blends is the most populous group of all. In this case, blends composed by two polymers are characterized by the presence of two phases.

Generally polymers tend to form biphasic systems. This is explained considering that the increase of entropy associated with the mixing isn't enough to balance the unfavourable interactions between different chains.

To form homogeneous mixtures it is necessary that intermolecular interactions between different chains are allowed, that molecular parameters like viscosity and molecular weight are appropriate and that the experimental conditions used while preparing the blends are the correct one [22].

As said before most of commercial polymer blends are formed from immiscible components. There are procedures, such the addition of compatibilizing agent, to make blends more miscible ("compatible"). Other technique to obtain miscible blend is to lower the interfacial energy between the two polymers and reducing coalescence. This is very important because with these techniques it is possible to increase the mechanical properties of the mixture.

Usually as compatibilizers are used macromolecules able to provide molecular interactions, such as covalent or ionic bonds, hydrogen bonds or chemical reactions at the interface between the polymers. These phenomenon are able to reduce the surface tension bringing a better dispersion of one component in the other and promoting the adhesion between the two phases [23].

Compatibilization could be divided into two categories:

- *ex situ*, a pre-synthetized copolymer is added to the blend. This is very useful because it allows to have an easy control on both the architecture of the blend and the compatibilizer.

  The most used compatibilizing agent are block copolymers or grafted copolymers which present segments with good affinity to the polymers that form the blend.
- *in-situ*, in which a copolymer is formed during the preparation of the blend. One of the most studied way to compatibilize blends with this method is the mixing reagent. This technique is used on blends formed by two polymers because, with more components, the complexity of the system and the number of the variables that need to be considered (different interphases, viscosity of the component and of the complete system, the chemical structure and reactivity of every component) make the study very complex.

  The objective of this technique is to compatibilize the component by generating directly at the interface the compatibilizing agent.

PLA and PCL are immiscible, even if not highly incompatible [24]; therefore considerable efforts have been made in order to obtain a fine dispersion of the phases of mixed homopolymers, to create structures with good mechanical characteristics and obtain PCL domains with reduced dimensions, so as to increase the contact surface between the phases.
In previous studies is reported how different organoclays are able to perform an emulsifying action in the PCL and PLA/PCL blends reducing the dimension of the PCL domains [25].
In this study we decided to try two different way to enhance the miscibility of PLA and PCL: using MMT30B and using MMT30B-g-P(LLA-co-CL).After the prepararion of the blends we are able to evaluate if these components are able to modify the crystallization rate of PLA which is the main focus of this work.

1.5 Crystallization

Crystallization of polymers is a process associated with partial alignment of their molecular chains. To obtain the crystallization of the polymer the chains required to have some characteristics:

- Regular constitutional units (unit's repetition must be equal and have the same chaining);

- Regular configuration (presence in the polymer of stereoregularity due to the use of monomers with identical spatial configuration);
- Regularity of conformation (regular repetition of the structural elements along the axis of the chain and representable by means of a helix).

If these characteristics are respected the chains fold together and form ordered regions called lamellae, which compose larger spheroidal structures named spherulites.

Polymers are composed by very long chains with the presence of imperfection on it. These imperfections as well as the high molecular weigh don't allow a complete crystallization of the polymer; in fact, the degree of crystallinity is estimated by different analytical methods and it typically ranges between 10 and 80%, thus crystallized polymers are often called "semicrystalline".

Polymers can crystallize upon cooling from the melt, mechanical stretching or solvent evaporation. Crystallization affects optical, mechanical, thermal and chemical properties of the polymer. The properties of semicrystalline polymers are determined not only by the degree of crystallinity, but also by the size and orientation of the molecular chains. For these reasons is very useful to study the crystallization behavior of a polymer to design the correct compound for the applications required.

The basic unit of a crystal is called "lamellae" and it is formed when different segments of the chains are parallel to each other. The stability of a lamellae is enhanced by the regularity mentioned before for the molecular chains which is the cause of the formation of good intermolecular interactions.

When the crystallization starts from the melt, the polymer superstructure arranges into spherulites.

Spherulitic morphology is formed by the grow in all the directions of the lamellae starting from a central nucleus of crystallization. All the voids are filled homogeneously thanks to a mechanism of lateral branching [26].

Generally, crystallization's temperature is included between 30°C above the glass transition temperature (Tg) and about 10°C below the melting temperature (Tm) [27].

When the temperature of crystallization (Tc) is near to the Tm the structure of the macromolecules can reach a high mobility which enhances the activity of the chains passing from an ordered structure to a disordered one favouring the formation of bigger crystals.

When the Tc is close to the Tg it is possible to affirm that the system has a high viscosity and the chains have lower mobility in comparison with the case above mentioned leading to the formation of small crystals.

Crystal melting is the process in which the polymer chains are forced to loose the ordered crystalline structure and turns into a pell-mell liquid.
Melting temperature (Tm) of the crystals depends on molecular weight, on the thermal history and on the crystallization temperature (Tc).

1.6 Crystallization kinetics

The development of the crystalline phase requires two consecutive processes: the formation of nuclei or primary crystallization (I) in the amorphous phase and their growth or secondary crystallization (G) in which there is the formation of stable nuclei on the surface of the growing crystal and their subsequent development.
Nucleation can be divided into homogeneous nucleation and heterogeneous one. It is defined homogeneus when it is present the sporadic formation of critical nuclei from the pure phase. It is defined heterogeneus when it occurs at the surface of impurities within the system [27].This last process is the most common.
Considering the time scale in which the nucleation process occurs, it can be classified as:

- Instantaneous, when many spherulites of small size due to the formation of many nuclei in the same instant are formed. It is obtained to high supercooling (i.e. the difference between the melting temperature of the crystals and the temperature of crystallization, $\Delta T = T_m - T_c$) where the nucleation rate is greater than the growth rate of the crystals.
- Sporadic when the growth rate is higher than the nucleation rate. In this case a few large spherulites can be observed using low values of supercooling.

The rate of growth of the crystals is connected to a rearrangement of the crystalline phase already formed or a subsequent crystallization of polymer segments of the amorphous phase, which brings an increase in the amount of crystalline fraction.
Figure 1.6 shows the trend of the primary nucleation rate (I) and of the rate of crystal growth (G) with the temperature. Both the curves present a bell-shaped trend, and both are included between Tg and Tm.

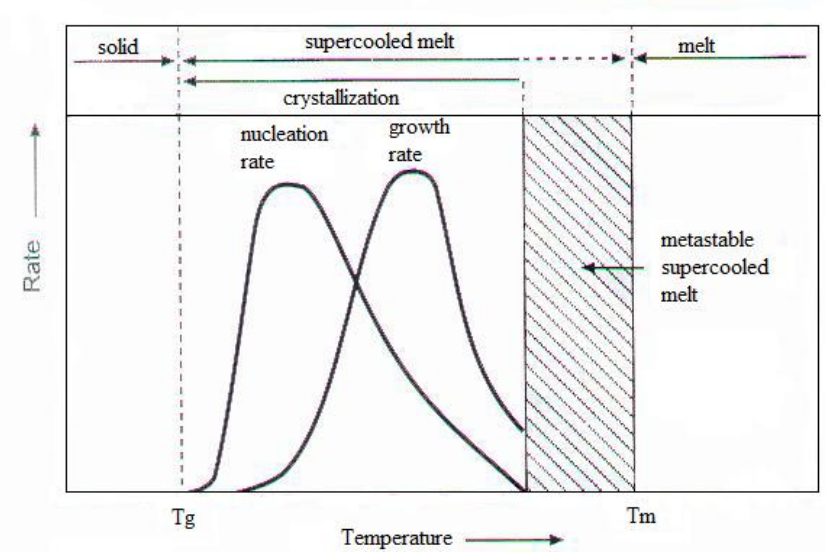

Figure 1.6 Temperature dependence of the nucleus formation rate and the crystallite growth rate on cooling from the melt[28].

The trend of the crystallization growth rate depends only on the crystallization temperature , instead of the nucleation rate which depends on various conditions such as the cooling rate from the molten state.

The overall rate of crystallization is given by the contribution of both rate (I) and (G). The temperature of crystallization is very important since it determines the thermal energy of the macromolecules: at higher temperatures the crystallization rate is slow and the process is controlled by the nucleation because of the greater mobility of the polymer chains. Lowering the temperature, the crystallization rate increases, it reaches a maximum and then it decreases when the crystallization process is controlled by diffusion, which is hindered at low temperatures.

Figure 1.7 shows that the overall crystallization rate presents a maximum at intermediate temperatures. This is due to the fact that temperature has opposite effects on both the rate of diffusion and deposition.

Also molecular weight is an important parameter that must be considered studying the crystallization rate. In fact a similar trend to the one above mentioned could be seen conparing crystallization rate and molecular weight. A bell-shaped trend is obtained with a maximum at intermediate molecular weight. In fact, primary nucleation rate increases with the increase of the molecular weight, while the growth rate has an opposite behavior.

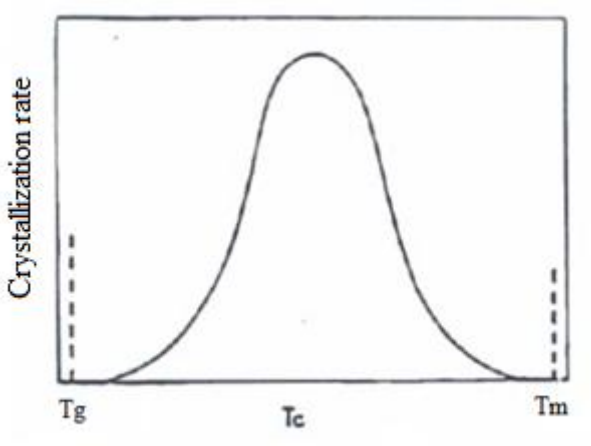

Figure 1.7 Crystallization rate vs. crystallization temperature.

Analyzing the growth rate (shown in Figure 1.8) as a function of the molecular weigh, if the polymer has a high molecular weight, we have an increase of the crystallization temperature corresponding to the high crystalliyzation rate; inversely, low molecular weight polymers require less time and lower temperature to crystallize. This is due to the fact that high molecular weights slow down the diffusional processes. Considering nucleation, high molecular weight contributes to the stability of the nuclei [29].

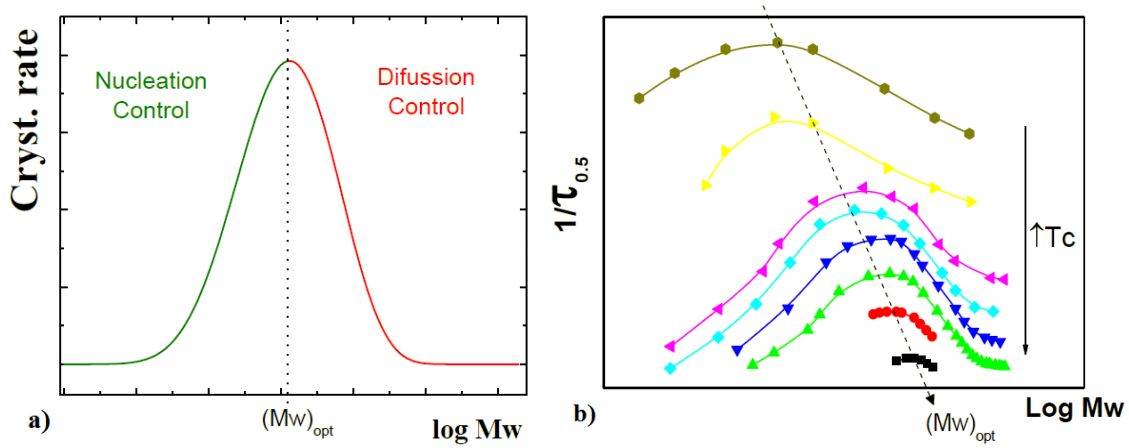

Figure 1.8 a) Overall crystallization rate vs the mass logarithm at T = const. b) The overall crystallization rate ($1/\tau_{0.5}$) vs. the mass logarithm for different temperatures [29].

1.6.1 Avrami theory

Avrami crystallization theory is applicable to explain the crystallization of polymers, even if originally it was used for compounds with low molecular weight. It allows to obtain

information on the process measuring the development of crystallinity at a constant crystallization temperature.

In this work it has been used to evaluate how overall crystallization rate change in the blends containing nanofillers.

Both the nucleation process and crystal growth are evaluated with this theory and as a result it is obtained a good experimental data during the primary crystallization range, up to approximately 50% conversion from amorphous to crystalline phase.

According to Avrami theory of crystallization, the progress of the isothermal crystallization could be expressed by the following equation [27]

$$1 - Vc = \exp\left[-k(t - t_0)^n\right] \qquad \text{Equation 1.1}$$

Where V_c is the crystalline volume fraction of the material, k is the constant rate of the overall crystallization (both nucleation and growth), t_0 is the induction time and n is the Avrami index that is obtained by:

$$n = n_d + n_n \qquad \text{Equation 1.2}$$

Where n_d is connected to the size of the growing crystal and could reach three values (1,2,3) which represent the one - two- or three dimension of the crystal. Usually analyzing polymers n_d falls in the values between 2 and 3 which indicate an axial representation (aggregated lamellae) or spherulites.

n_n describes the process of nucleation and consists of two values 1 and 0: 0 for instantaneous nucleation and 1 when sporadic nucleation occurs.

V_c can be calculated with the equation:

$$Vc = \frac{Wc}{Wc + \frac{\rho_c}{\rho_a}(1 - Wc)} \qquad \text{Equation 1.3}$$

$$Wc = \frac{\Delta H_{(t)}}{\Delta H_{tot}} \qquad \text{Equation 1.4}$$

where ρ_a and ρ_c correspond to the density of completely amorphous and completely crystalline polymer respectively; $\Delta H_{(t)}$ corresponds to the enthalpy of crystallization as a function of the crystallization time, while ΔH_{tot} is the overall isothermal crystallization enthalpy of the material.

Re-elaborating Equation 1.1 by applying logarithmic properties brings to the following equation:

$$\log [-\ln (1 - Vc)] = \log (K) + nlog(t - t_0) \qquad \text{Equation 1.5}$$

This equation is very useful because it allows to graphically extract both *n* and *K* plotting $log[-ln(1 - Vc)]$ with the $nlog(t - t_0)$ function.
Time required by the polymer studied to reach the 50% of crystallization can be indicated with both $\tau^{1/2}$ or $\tau_{50\%}$ obtaining the following equation [27]:

$$\tau_{1/2} = \left(\frac{-\ln (1-Vc)}{k}\right)^{1/n} = \left(\frac{-\ln (0.5)}{k}\right)^{1/n} \qquad \text{Equation 1.6}$$

1.6.2 Lauritzen Hoffman theory

The quantitative model of Lauritzen-Hoffman (L-H) is used to predict the crystal growth rate (G).
The crystal growth rate (G) is governed by two important processes that are a function of the rate (*i*) at which the nuclei are formed and the rate (g) at which the nuclei spread on the surface of the crystal. Depending on which of the two rate is higher, we can be in three different crystallization regimes ; I, II, III:

- Regime I is obtained in the presence of a low supercooling value and when the nucleation rate is smaller than that of growth;
- Regime II is obtained when the temperature decreases bringing an increase in the nucleation rate and a decrease in the rate of growth;
- Regime III is obtained in the presence of a large supercooling value and when the nucleation rate is higher than that of growth rate [30].

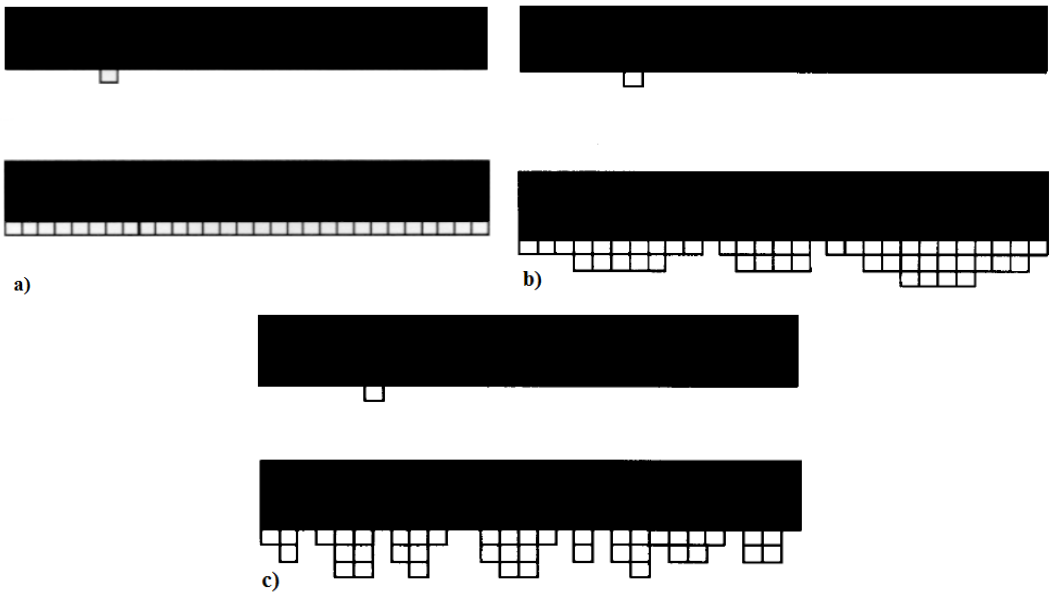

Figure 1.9 Schematic drawings of how polymer crystal growth takes place in three regimes: a) regime I, b) regime II, and c) regime III [31].

According to the L-H theory, the rate of crystal growth could be described by the following equation: [38,40]

$$A(T) = A_0 \, exp\left(\frac{-U^*}{R(T_c - T_\infty)}\right) exp\left(\frac{-K_g^A}{T_c - \Delta T f}\right) \qquad \text{Equation 1.7}$$

The equation is divided into two parts: the first exponential represents the spread of the chains for the growth process, while the second describes the energy barrier of the secondary nucleation.

A_0 represents a pre-exponential parameter of the rate of growth, U^* is the activation energy for the chains mobility, R is the universal gas constant, Tc is the temperature of isothermal crystallization, $\Delta T = T_m^0 - Tc$ is the supercooling (T_m^0 is the equilibrium melting temperature), $T_\infty = Tg - 30$ is the hypothetical temperature where all motion are locked and f is a defined correction factor of the temperature:

$$f = \frac{2T_c}{(T_m^0 + T_c)} \qquad \text{Equation 1.8}$$

K_g^A is the nucleation rate constant, which is proportional to the energy barrier for secondary nucleation and is represented by the following equation:

$$K_g^A = \frac{jb\sigma\sigma_e\ T_m^0}{k_B\ \Delta H_m}$$ Equation 1.9

Where j is a constant which depends on the regime of crystallization and it can assume different values for regimes I and III, while it is always 2 for regime II, b is the layer thickness, k_B the Boltzmann constant (1,3806503x10^{-29} J/K), ΔH_m is the melting heat, σ_e is the free energy of folding and σ is the lateral surface free energy.

Figure 1. 10 shows the plot of $\ln(G) + U^*/R(T_c - T_\infty)$ as a function of $\frac{1}{T_c \Delta T}$ from which it is possible to determine K_g^A [31].

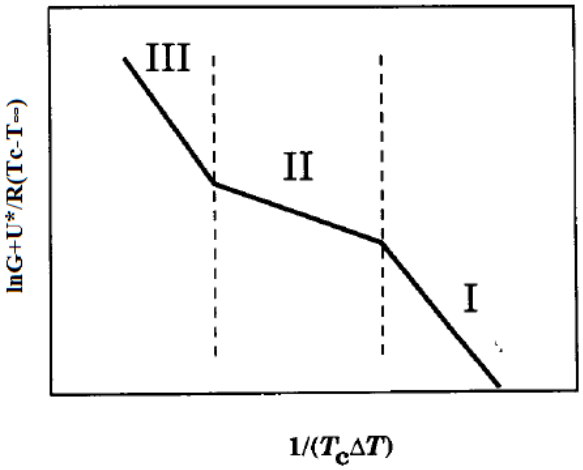

Figure 1.10 Growth rate regimes [31].

By using the L-H theory other two parameters could be calculated σ_e and q which is the work required for chain bending, using the equations [30]:

$$\sigma = 0.1\ \Delta H_m^0 \sqrt{a_0\ b_0}$$ Equation 1.10

$$\sigma\sigma_e = \frac{K_g\ \Delta H_m^0}{jb_0 T_m^0}$$ Equation 1.11

Where a_0 is the projection of the chain's longitude, b_0 the width of the chain both depending on the nature of the polymer

$$q = 2a_0 b_0 \sigma_e$$ Equation 1.12

2 AIM OF THE WORK

An important parameter that must be evaluated to clearly understand the behavior of PLA is its crystallization rate. A high rate is required to enhance PLA develop in the industry, indeed the great interest on this biodegradable and biocompatible polymer find its major problem in the slow crystallization rate.

Industry still prefer to use other polymers because they reach higher crystallinity than PLA considering the same processing time. The low crystallization rate is connected with the poor mobility that the macromolecules chains have and moreover PLA with low level of crystallinity presents low thermal resistance [2].

Both inorganic and organic nanocomposites are used as a remarkable solution to enhance the crystallization rate of PLA because they could act as heterogeneus nucleant. Furthermore there are used to improve mechanical and phisical properties when PLA is blended with other polymers [2].

The use of nanoclay such as montmorillonite is reported in many studies as an efficient way to enhance the crystallization of PLA [32]. However to improve its effect, a good compatibility between nanoclay and PLA is required. An interesting approach to reach this result is given by the possibility to insert, in the structure of the MMT, organic components with a process of ion exchange. Adding an organic functionality to the MMT cause an increase in organophilicity of the clay and a further chance to enhance the compatibility with PLA due to the exfoliation and dispersion of the clay. In this study thanks to "*the grafting from*" approach a good degree of exfoliation and high grafting density of organoclay are obtained.

In this work the effect of organoclay dispersed in PLA/PCL blends on the PLA crystallization rate will also be investigated.

Two different nanofillers were evaluated and compared: neat MMT30B and MMT30B with grafted poly(L-lactide-co-ε-caprolactone). The second one was synthetized through a technique called Surface-Initiated Ring Opening Polymerization (SI-ROP) in the presence of tin(II) octoate [$Sn(Oct)_2$] as a catalyst and the hydroxyl groups of the ammonium salt present on the organoclay as initiators.

Blends were prepared by solvent casting and then characterized by SEM, TGA and DSC. SEM analysis were performed to evaluate how the two different nanofillers could affect the morphology of PLA and PCL in the blends.

TGA analysis were used to evaluate the effect of the nanofillers on the thermal stability of the blends.

DSC analysis were used to measure the effect of the nanofillers on the thermal properties of the polymeric matrix. The overall crystallization rate of PLA was investigated by both isothermal and non-isothermal DSC.

3 RESULTS AND DISCUSSION

Organoclay based nanofillers were successfully synthetized by the *in situ* grafting reaction of the random copolymer poly(lactide-ran-caprolactone) P(LA-ran-CL) on montmorillonite (MMT30B). The synthesis was carried in xylene at 140°C, as suggested by the results of a solvent and temperature screening.

The composition of the grafted copolymers on the organoclay were evaluated by ^{1}H-NMR (Hydrogen Nuclear Magnetic Resonance Spectroscopy) whereas the amount of clay in the nanofiller was evaluated by ATR–IR (Attenuated Total Reflection Infrared Spectroscopy) and TGA (Thermogravimetric Analysis).

Solvent casted films were achieved by solution mixing the nanofillers with neat poly(lactide) PLA or poly(lactide)/poly(caprolactone) PLA/PCL blends, comparing the properties with the PLA and PLA/PCL blends containing the unmodified clay.

The films were evaluated by SEM (Scanning Electron Microscopy), DSC (Differential Scanning Calorimetry) and TGA (Thermogravimetric Analysis).

These analysis were foundamental to notice that the nanofillers used are immiscible with the PLA matrix and that PLA and PCL are immiscible even if the grafted copolymer causes a better dispersion of PCL in PLA matrix.

Moreover it was observed that nanofillers act reducing the thermal stability of the blends but we were also able to promote the increase of the crystallization rate of PLA. The same increase of rate was observed in blends containing PCL.

Finally Avrami index was used to evaluate the isothermal crystallization rate and no differences in the behavior of PLA were noticed respect to previous studies [33].

3.1 Synthesis and characterization of the MMT30B-g-P(LA-ran-CL)

Poly(lactide-ran-caprolactone) grafted on montmorillonite 30B (MMT30B-g-P(LA-ran-CL)) was synthesized by Surface Initiated Ring Opening Polymerization (SI-ROP) of D,L-lactide and ε-caprolactone on MMT30B. By this technique the polymerization is started on the hydroxyl groups of MMT30B, upon the effect of a Lewis acid catalyst, as tin(II) octoate ($Sn(Oct)_2$) [34](Figure 3.1).

To obtain the required product a screening on the reaction conditions was performed. In this screening were evaluated the amount of reactants ideal for the reaction, the temperature at which perform the synthesis, time of reaction and the possible use of a solvent. Every product

was evaluated by ^{1}H-NMR technique and by TGA analysis to estabilish which reaction gave the best result.

After the screening the reaction which gave the best copolymer grafted to the organoclay was scaled up to produce the amount of product needed for the successive experiments.

It's important to underline that during the synthesis part of the copolymer formed didn't react with MMT30B. This product was separated and used to determine the composition of the copolymer with ^{1}H-NMR analysis.

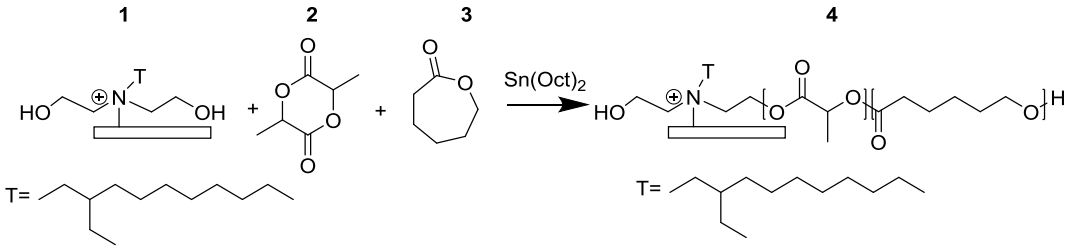

Figure 3.1: Synthesis of the MMT30B-g-P(LA-ran-CL) **(4).** D,L-Lactide **(2)** and ε-Caprolactone **(3)** were loaded at the same amount, while MMT30B **(1)** following the results of the screening test.

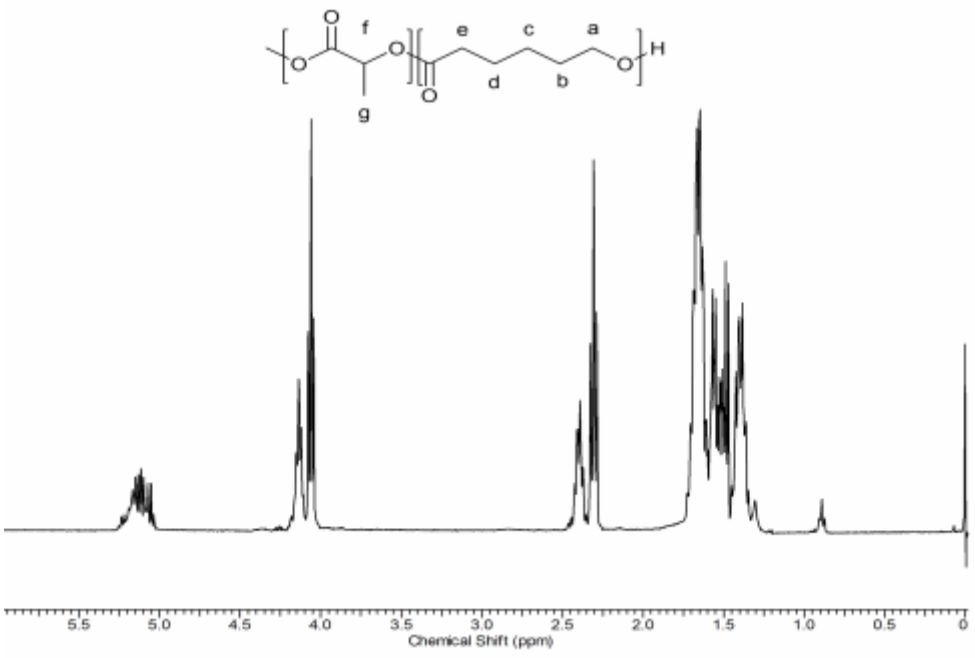

Figure 3.2: H^{1}-NMR spectrum (400 MHz, $CDCl_3$) and chemical structure of the P(LA-*ran*-CL) random copolymer

3.1.1 Characterization of the MMT30B-g-P(LA-ran-CL)

The composition of grafted P(LA-ran-CL) was determined by ^{1}H-NMR analysis.

Since MMT30B-g-P(LA-ran-CL) is not soluble in any solvent, the non-grafted P(LA-ran-CL) was taken as reference, being confident in the hypothesis that the grafted and the non-grafted copolymer chains have the same composition [34].

In Figure 3.2 the ^{1}H-NMR spectrum of non-grafted P(LA-ran-CL) is presented. For the assignment of the polymer characteristic signals the work of Peponi et al. [35] was taken as reference. The multiplet from 5.05 to 5.25 ppm is assigned to methine proton of polymerized lactide unit (LA) (f). The multiplet from 4.08 to 4.18 ppm is due to the caprolactone unit (CL) protons (a) that are linked to a LA molecule, while the triplet at 4.05 ppm indicates that the CL protons are linked to another CL molecule. The multiplet between 2.34 to 2.44 ppm is due to the CL protons (e) that are linked to a LA molecule, while the triplet at 2.30 indicates that the CL protons are linked to another CL molecule. For the rest of the spectrum, multiplets at 1.66 ppm and 1.39 ppm are related to the CL protons (b), (d), and (c), respectively, and the multiplet at 1.56 ppm, to the LA methyl protons (g). So, the ratio of the LA signals to the CL signals results in a molar composition of the copolymer.

The amount of clay in MMT30B-g-P(LA-ran-CL) nanofillers was estimated by TGA.

In Figure 3.3 are presented the thermograms of MMT30B-g-P(LA-ran-CL) nanofillers (called as MMT30BCLLA5050) and neat MMT30B. The measurements were conducted in a nitrogen atmosphere, by a 20°C/min heating ramp from 40 °C to 600 °C. Thermograms of MMT30B shows, between 270°C and 470°C, a 25.6% mass loss due to the ammonium salt present in the functionalized clay (see Figure 3.3). In MMT30B-g-P(LA-ran-CL) the loss between 270°C and 470°C is due to the total organic fraction of the nanofiller, since the loss of ammonium salt is overlapped with the grafted P(LA-ran-CL) chains degradation.

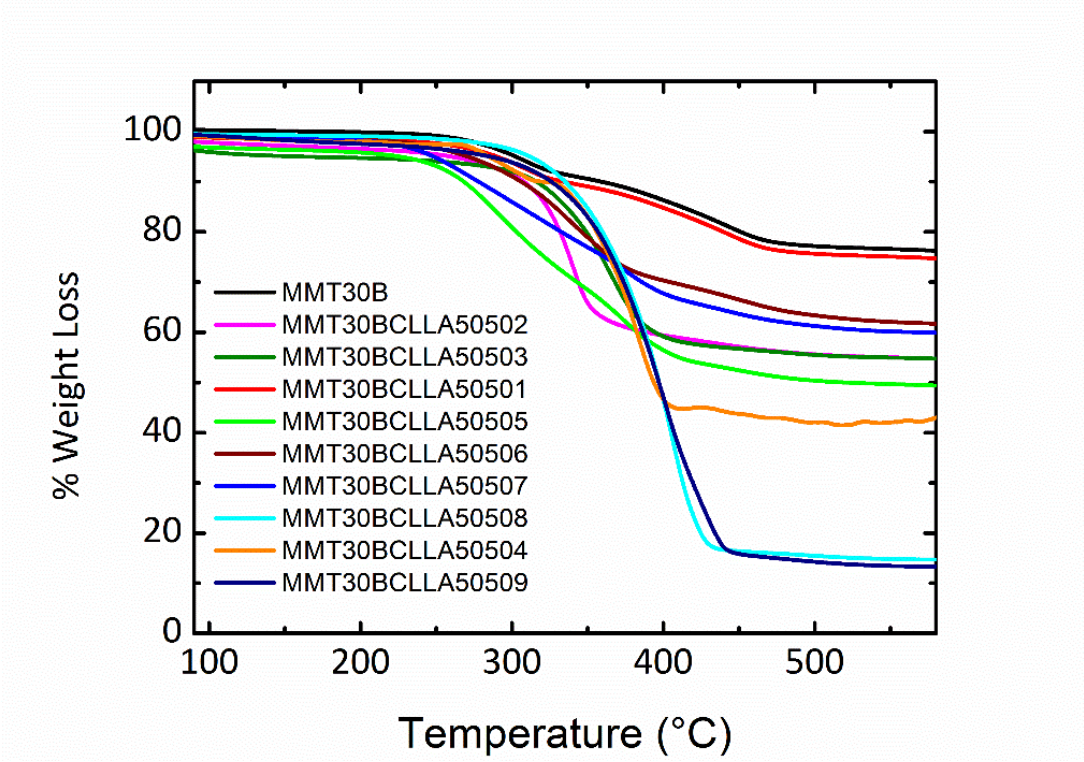

Figure 3.3: Thermograms of MMT30B and MMT30B-g-P(LA-ran-CL) nanofillers (called as MMT30B5050CLLA). The measurements were conducted in a nitrogen atmosphere, by a 20°C/min heating ramp from 40 °C to 600 °C

3.1.2 Screening of the parameters for the synthesis of the MMT30B-g-P(LA-ran-CL)

To be useful for blending with PLA or PLA/PCL, MMT30B-g-P(LA-ran-CL) must be synthesized in order to obtain a precise architecture. We are confident that the amount of clay must be around 10% w/w, in order to increase the dispersion in the polymer matrix during the blending. Furthermore, to act as compatibilizer agents, the grafted P(LA-ran-CL) chains must contains the same amount of lactide (LA) and caprolactone (CL) units, linked in a random sequence. Our hypothesis follows previous works in which similar nanofillers were used [36]. Therefore D,L-lactide and ε-caprolactone were loaded at the same molar amount, while the amount of the clay and the catalyst, the time, the solvent and the temperature of the procedure were chosen upon the results of screening tests (Table 3.1).

Initially, the reaction was carried out at 120 °C in bulk, since reactions without any solvent could ensure a lower cost and environmental impact if compared with the equivalent in

solvent. The temperature of 120°C was chosen since it lies in the middle between the melting (95°C) and degradation (140°C) temperature of D,L-lactide.

Notwithstanding our confidence in choosing these conditions is also supported by previous works reporting P(LA-ran-CL) polymerization [37], first tests shows that the addition of clay have a dramatic effect on the reaction; in fact, an increasing of the reaction media viscosity and therefore a reduction of the dispersion of the reactants was observed.

As results, Table 3.1 shows that loading a clay amount of 1.9% (MMT30BCLLA50501) the grafting reaction does not proceed. Decreasing the loading to 1% (MMT30BCLLA50502-3) better results are obtained. However, being confident that solvent addition would have further improved the dispersion of the clay in the reaction media, we decided to carry out the reaction in toluene.

Table 3.1 Starting data and results of interest in screening reactions

Sample	Procedure					Results	
	MMT30B (w/w %)	**Cat. (mol/mol %)**	**Time (h)**	**Temp. (°C)**	**Solvent**	**MMT30B (w/w %)[1]**	**LA Copolymer composition (mol/mol %)[2]**
MMT30BCLLA50501	1.9	0.2	48	120	-	100	54
MMT30BCLLA50502	1.0	0.1	48	120	-	55	46
MMT30BCLLA50503	1.0	0.1	48	120	-	55	45
MMT30BCLLA50504	1.0	0.1	24	120	-	42	48
MMT30BCLLA50505	1.0	0.1	24	85	Toluene	50	80
MMT30BCLLA50506	1.9	0.2	24	85	Toluene	62	79
MMT30BCLLA50507	3.8	0.5	24	85	Toluene	60	41
MMT30BCLLA50508	1.0	0.1	24	120	Xylene	15	51
MMT30BCLLA50509	1.9	0.2	24	120	Xylene	13	48

[1] = Determined by TGA, taking neat MMT30B as reference

[2] = Determined by ^{1}H-NMR on the non-grafted copolymer fraction

The choice of toluene as solvent, (b.p 113 °C), implies a reduction in temperature from 120°C to 85°C. Since our reaction Schlenk flask, is not designed for working at high pressures. Reaction time was reduced from 48h to 24h, since no significant change were noted passing from MMT30BCLLA50503 to MMT30BCLLA50504.

The choice of carring out the reaction in a solvent has proved satisfactory. In fact, raising the amount of clay from 1% to 3.8% (MMT30BCLLA50505-7) no significant differences in the amount of grafted polymer were noted.

However the results in Table 3.1 show that the temperature reduction from 120°C to 85°C implies a change in polymer composition probably due to a change in the reactivity rates. Looking at MMT30BCLLA50505-7 is it possible to observe that, despite D,L-lactide and ε-

caprolactone were loaded at the same molar amount, the composition of P(LA-ran-CL) is enriched in lactide unit (LA% mol/mol). It basically means that at 85 °C D,L-lactide is more reactive than ε-caprolactone and the choosen composition (50% LA-50%CL) it is more difficult to achieve.

It was decided to change the solvent from toluene to xylene (b.p 140 °C), re-increasing the reaction temperature from 85°C to 120°C. This choice ensures at the same time a comparable reactivity of the two monomers and a good dispersion of the clay.

As Table 3.1 show, the last grafted copolymers have the desired composition (around 50% LA-50%CL), and the amount of clay is reduced to 13-15% meaning an effective clay functionalization.

3.1.3 Synthesis of the MMT30B-g-P(LA-ran-CL)

Taking into account the information achieved by the screening of the parameters, the synthesis of the MMT30B-g-P(LA-ran-CL) was carried out in xylene at 120°C, using MMT30B5050CLLA9 (Table 3.1) as reference and scaling up all reactants five times, in order to obtain the amount of nanofiller required for the blend preparation. In Table 3.2 are reported the parameters and the results obtained. The amount of grafted polymer was calculated by the following formula:

Copolymer (w/w %) = 100 - MMT30B (w/w%) * (1 + A.M%) Equation 3.1

where MMT30B represents the total amount of the clay and A.M% is the amount of the ammonium salt in the organoclay. This value was set at 26% after its determination with TGA analysis (Figure 3.3).

For our product it was found with TGA that the amount of MMT30B was 30% (w/w) and that the copolymer grafted on it was 62% (w/w). With ^{1}H-NMR analysis on the non-grafted copolymer it was found that the LA copolymer composition was 45% (mol/mol)

The decreases of the grafted copolymer amount in MMT30B5050CLLA, in comparison with MMT30B5050CLLA9, is due to the scale up. Increasing all reactants five times but carrying out the reaction by the same stirring system a worse dispersion of the clay is obtained.

In any case, in order to achieve clear information on the structure of the product before the blending, ATR–IR was registered. Figure 3.4 shows the IR spectrum of MMT30B5050CLLA in comparison with neat MMT30B.

In MMT30B, the presence of peaks at 3635 cm^{-1} and 2925 cm^{-1} are respectively related to the -OH and -CH_2 groups of the ammonium salt.

The presence of the grafted polymer in MMT30B5050CLLA is confirmed by the peak at 1735 cm^{-1} related to C=O of both LA and CL units and by the peak at 1030 cm^{-1} related to the C-O-C bonds.

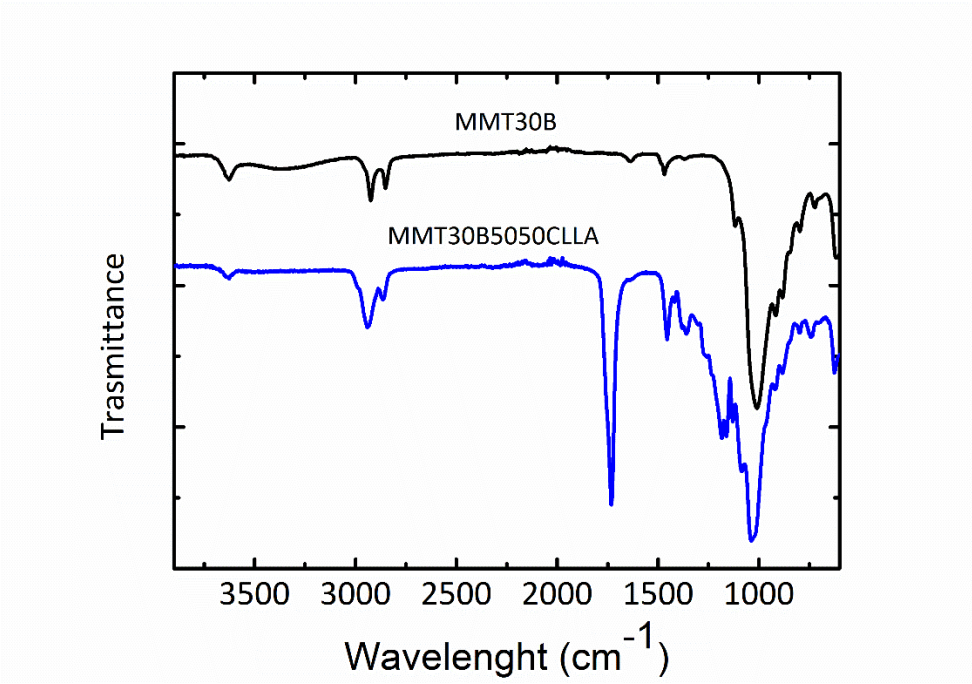

Figure 3.4 ATR-IR spectrum of MMT30B and MMT30B5050CLLA from 4000 cm^{-1} to 500 cm^{-1}.

3.3 Blend preparation

Solvent casted PLA/PCL blends, with and without MMT30B or MMT30B-g-P(LLA-co-CL) were prepared. PLA/PCL were mixed at a constant weight ratio of 80/20, while nanofillers were added at 5% w/w. The composition of each sample is listed in Table 3.2.

The blends were prepared by dissolving PLA, PCL and the nanofillers in chloroform at room temperature. PLA/PCL/nanofillers film were obtained from 1w% solution in chloroform. The films were dried for 24 hours at room temperature and for 24 hours into an oven at 60°C to completely remove the solvent [33].

To enhance the solubilization of the nanofillers inside the polymeric matrix the solutions were sonicated for 60 minutes even if this process could possibly result to a chain breaking with consequent reduction of the molar weight.

Table 3.2 (w/w %) of PLA, PCL and nanofillers in each blend

Sample	PLA (w/w%)	PCL (w/w%)	MMT30B (w/w%)	MMT30B-g-P(LLA-co-CL)(w/w%)
PLA	100	-	-	-
PLA/PCL 80/20	80	20	-	-
PCL	-	100	-	
PLA/MMT30B 100/5	95.2	-	4.8	-
PLA/PCL/MMT30B 80/20/5	76.2	19	4.8	-
PCL/MMT30B 100/5	-	95.2	4.8	-
PLA/MMT30B-g-P(LLA-co-CL) 100/5	95.2	-	-	4.8
PLA/PCL/MMT30B-g-P(LLA-co-CL) 80/20/5	76.2	19	-	4.8
PCL/MMT30B-g-P(LLA-co-CL) 100/5	-	95.2	-	4.8

The blends were studied by:

- Scanning Electron Microscopy (SEM), in order to evaluate their morphology and therefore the miscibility between PLA and PCL and the effects of the nanofillers.
- Thermogravimetric Analysis (TGA), in order to analyze the thermal stability of the samples.
- Non-isothermal Differential Scanning Calorimetry (DSC), in order to evaluate the non-isothermal melting and crystallization behavior of PLA and PCL upon the effects of the nonofiller
- Isothermal DSC in order to evaluate the isothermal crystallization behavior of PLA upon the effect of the blending and the nanofiller addition

3.4 SEM micrographs

Figure 3.5 shows SEM micrographs for cryogenically fractured surfaces of PLA/MMT30B and PLA/MMT30B-g-P(LLA-co-CL). The nanofillers appear as white particles, immiscible with the matrix. It seems that MMT30B it is aggregated into larger particles compared to MMT30B-g-P(LLA-co-CL). This behavior it's correlated to the better exfoliation of the clay laayers in MMT30B-g-P(LLA-co-CL) upon the effect of the grafted random copolymer. In fact, as reported in literature [1], the in-situ polymerization increases the space between the interlayers of the clay allowing a better exfoliation. Dubois et al. [36] [38] and Thomas,

McLauchlin [39] demonstrated the intercalation of PLA or PCL in the structure of modified montmorillonite by WAXS and TEM analysis.

Figure 3.6 shows SEM micrographs for cryogenically fractured surfaces of PLA/PCL, PLA/PCL/MMT30B and PLA/PCL/MMT30B-g-P(LLA-co-CL).

PLA/PCL blends shows the typical *sea-island* morphology typical of immiscible blends. PLA conforms to the matrix while PCL is finely dispersed as droplets. The immiscibility of PLA/PCL blends has been well documented. Wu et al. [40], studying PLA/PCL blends at different composition reported that the blend morphology changed from fibrillar for the 60/40 composition to spherical for the 80/20 composition.

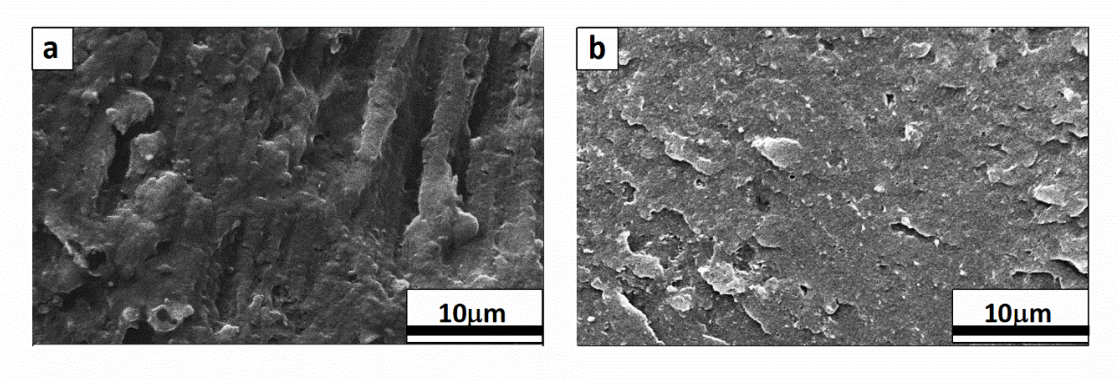

Figure 3.5 Scanning Electron Microscope (SEM) images of a) PLA/MMT30B 100/5 and b) PLA/MMT30B-g-P(LLA-co-CL) 100/5 blends

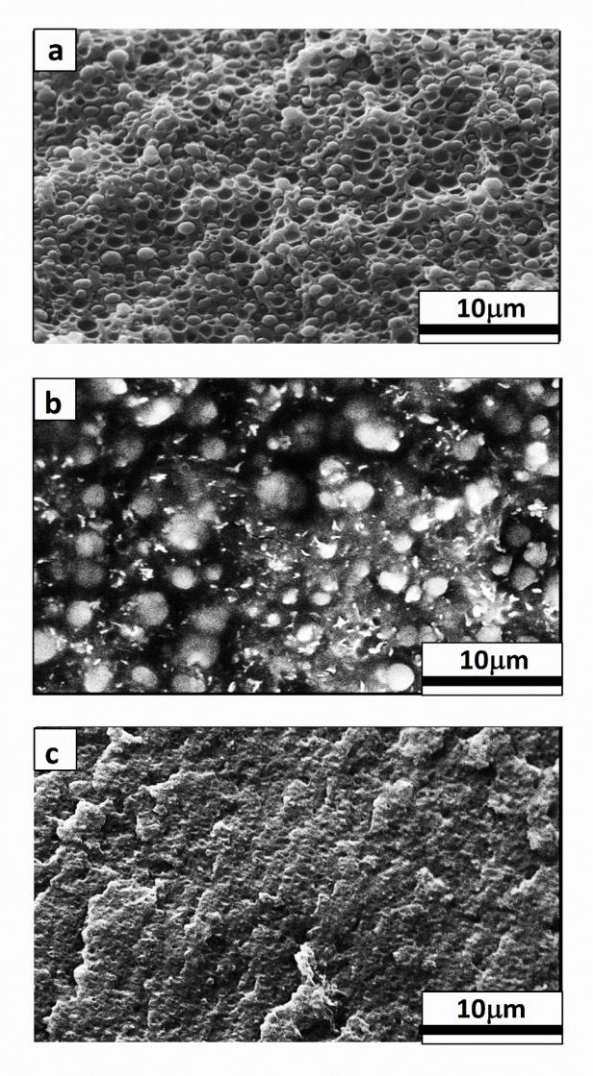

Figure 3.6 Scanning Electron Microscope (SEM) images of a) PLA/PCL 80/20, b) PLA/PCL/MMT30B 80/20/5, c) PLA/PCL/MMT30B-g-P(LLA-co-CL) 80/20/5.

Table 3.3 reports average diameters and particle size distributions of PCL droplets in the blends. Number (d_n) and volume (d_v) average diameters and particle size polydispersity (D) were calculated by the following equations, by counting at least 50 PCL particles[41]:

$d_n = \sum n_i d_i / \sum n_i$ Equation 3.2

$d_v = \sum n_i d_i^4 / \sum n_i d_i^3$ Equation 3.3

$D = d_v / d_n$ Equation 3.4

Table 3.3 Data obtained analyzing SEM images of the PLA/PCL/nanofillers blend

Sample	n	dn (µm)	dv (µm)	D
PLA/PCL 80/20	100	2.15	2.42	1.13
PLA/PCL/MMT30B 80/20/5	50	3.57	3.92	1.09
PLA/PCL/MMT30B-g-P(LLA-co-CL) 80/20/5	50	1.25	1.41	1.12

Figure 3.6 clearly shows that PCL droplets in PLA/PCL/MMT30B 80/20/5 are bigger than in PLA/PCL 80/20. On the contrary in PLA/PCL/MMT30B-g-P(LLA-co-CL) 80/20/5 the PCL droplets are smaller than in PLA/PCL 80/20.

The same behavior is confirmed in Table 3.3 In PLA/PCL/MMT30B 80/20/5 the PCL particles are roughly two times bigger than in PLA/PCL 80/20 (dn 3.57 vs 2.15), while in PLA/PCL/MMT30B-g-P(LLA-co-CL) 80/20/5 the particles are quite smaller (dn 1.25 vs 2.15). It basically means that MMT30B-g-P(LLA-co-CL) can act as compatibilisers in the blend, promoting the compatibility between PLA and PCL.

We are confident that this behavior is correlated with the effect of copolymer grafted chains in MMT30B-g-P(LLA-co-CL). Indeed the copolymer grafted chains improve the interaction between the PLA and PCL phases, reducing the PCL particles size [1].

On the contrary, MMT30B cannot act as compatibilizer and therefore the PCL particle are increased in diameter.

3.5 Thermogravimetric Analysis (TGA) of blends

Figure 3.7 shows the thermograms of a) neat PLA, neat PCL and PLA/PCL 80/20 blends , b) PLA/MMT30B 100/5, PLA/PCL/MMT30B 80/20/5 and PCL/MMT30B 100/5 blends, c) PLA/MMT30B-g-P(LLA-co-CL) 100/5, PLA/PCL/MMT30B-g-P(LLA-co-CL) 80/20/5 and PCL/MMT30B-g-P(LLA-co-CL) 100/5, d) comparison of different PCL blends, e) comparison of different PLA/PCL blends and f) comparison of different PLA blends.

The Thermogravimetric Analysis on the blends were performed using High Resolution Technique. This technology is very useful because the heating rate is automatically varied by the rate of weight loss. In this way is it possible to highlight the weight loss of the samples, distinguishing also small differences. The analysis were conducted under nitrogen flow, by an heating scan from 40°C to 600°C.

In Table 3.4 are presented the data obtained from the thermograms. The temperature T_1 correspond to the temperature at which starts the first degradation of one component of the blend, T_2 is the second degradation that we encount during the analysis. Other temperatures reported are the temperature that the samples reach before reaching a 10% mass loss ($T_{10\%}$), the two onset temperature (T_{onset1} and T_{onset2}) and the residue at the end of the process.

The analysis were initially performed on the blends without nanofillers. Figure 3.7 a) shows that PLA degradates before pure PCL. This is attributable to the higher presence of carbonyl

groups in PLA than in PCL. In PLA/PCL 80/20 the PLA starts to degradate to a lower temperature respect to the one of neat PLA.

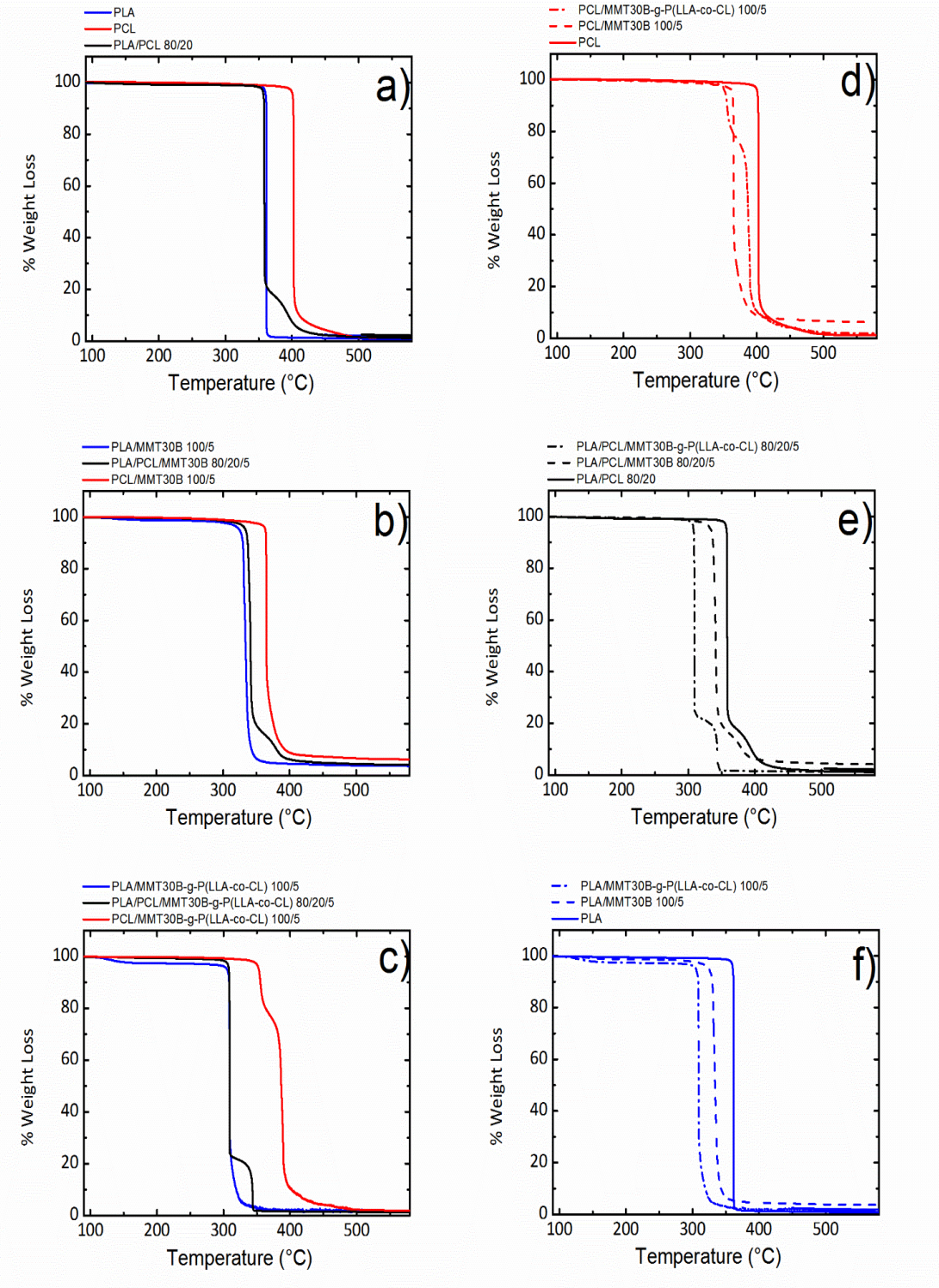

Figure 3.7 Thermogravimetric analysis of a) neat PLA, neat PCL and PLA/PCL 80/20 blend , b) PLA/MMT30B 100/5, PLA/PCL/MMT30B 80/20/5 and PCL/MMT30B 100/5blends, c) PLA/MMT30B-g-P(LLA-co-CL) 100/5, PLA/PCL/ MMT30B-g-P(LLA-co-CL) 80/20/5 and PCL/ MMT30B-g-P(LLA-co-CL) 100/5, d) comparison of different PCL blends, e) comparison of different PLA/PCL blends and f) comparison of different PLA blends.

Table 3.4 TGA data for PLA/PCL blends

Sample	T_{peak1} (°C)	T_{peak2} (°C)	$T_{10\%}$ (°C)	T_{onset1} (°C)	T_{onset2} (°C)	Resid. (%)
PLA	360.8		361.3	361.6		0.8
PCL	401.2		401.9	400.6		1.2
PLA/PCL 80/20	357.2	392.9	358.1	357.1	384.2	1.3
PLA/MMT30B 100/5	332.8		329.6	329.7		3.8
PCL/MMT30 100/5	363.5		364.6	364.8		6.3
PLA/PCL/MMT30B 80/20/5	340.3	378.8	337.1	336.3	385.4	4.3
PLA/MMT30B-g-P(LLA-co-CL) 100/5	307.6		308.3	308.5		1.2
PLA/PCL/MMT30B-g-P(LLA-co-CL) 80/20/5	308.0	343.5	308.7	308.9	342.6	1.3
PCL/MMT30B-g-P(LLA-co-CL) 100/5	355.2	387.9	355.3	352.4	383.5	2.0

MMT30B addition to the neat polymers implies a reduction of the samples thermal stability. Both Figure 3.7 d) e) f) shows that the blends without nanofillers are more stable than the blends containing nanofillers; in fact neat PLA degradation starts at 360.8°C, while PLA/MMT30B 100/5 and PLA/MMT30B-g-P(LLA-co-CL) 100/5 start respectively at 332.8 and 307.6°C. The same behavior is seen in blends of PLA/PCL and neat PCL.

Blends containing MMT30B were sonicated for 60 minutes to enhance the organoclay dispersion in the matrix. This procedure could lead to chain break of both PLA and PCL reducing molecular weight and thermal stability of the blends. Furthermore the montomorillonite can act as a catalyst in polyesters degradation, since the silicate layers surface of the clay are strongly acidic proton sites. [42].

MMT30B-g-P(LLA-co-CL) 100/5 further increases the degradation of the blends. It is possible that the presence of LiCl traces used to separate grafted organoclay from non-reacted one could act as a pyrolysis catalyst reducing thermal stability of blends.Furthermore the grafted copolymer chains, having a low molecular weight, could induce the degradation of the higher molecular weight neat polymer.

3.6 Differential Scanning Calorimetry (DSC): non-isothermal crystallization

Thermal properties as melting, crystallization and cold crystallization behavior of the blends were determined by DSC analysis.

Crystallization could be delayed or accelerated by the addition of PCL and of the nanofillers [43].

The samples were first heated to 200 ºC for 3 minutes in order to erase all crystalline thermal history. Then they were cooled at 10 ºC/min until -20 ºC while the corresponding cooling

scans were recorded. The last recording was taken when the samples were reheated to 200 ºC at the same rate to register the subsequent heating scans.

In Figure 3.8 are reported the data obtained by DSC scans performed on different samples. In Table 3.5 are reported the data obtained by these curves.

As shown in Figure 3.8 during the cooling from the melt state, neat PCL crystallizes at 28.4°C with a sharp exothermic peak.

In PLA/PCL/MMT30B-g-P(LLA-co-CL) 80/20/5 PCL phase is confined in small droplets (as seen from SEM analysis) and therefore the crystallization is fractionated into two peaks at 27.6 ºC and 15.8 ºC. Fractionated crystallization is a common occurrence in immiscible blends. It happens when the number of droplets of a crystallizable phase is larger or of the same order of magnitude as the number of active heterogeneities present in the bulk polymer before being dispersed [44].

PLA/PCL 80/20 and PLA/PCL/MMT30B 80/20/5 do not exhibit fractionated crystallization, since in this case PCL droplets are larger than in PLA/PCL/MMT30B-g-P(LLA-co-CL) 80/20/5 as seen in Figure 3.6 a) and b). Indeed, if the PCL droplets are larger, it is increased the probability to find an active heterogeneities nuclei which can activate crystallization within the droplets.

PLA does not crystallize during cooling at the scanning rate employed (10 ºC/min) in no one of the samples. The reason for this well-known behavior is the D-LA isomer content of 1.2-1.6 % present in PLA 4032D. D units act as defects to hinder the crystallization of L segments within the chains [43].

On the contrary, during the second heating scan PLA is able to develop a cold crystallization peak in every samples used. However, in neat PLA the peak is at 129.1°C while in the blends it is shifted at lower temperatures. It basically means that the blending of PLA with PCL promotes the cold crystallization. Recently, Sakai *et al.* proposed that in immiscible PLA/PCL blend a locally depressed glass transition temperature (Tg) of PLA at the interface with PCL domains can accelerate the nucleation of PLA during its cold crystallization[45]. However we are not confident with this hypothesis, since no detection of improved miscibility upon the blending is visible (non-significant variation of the PLA Tg are detected).

Instead we are confident that PCL could enhance PLA cold crystallization by a transfer of impurities, that acts as active heterogeneities, at the interface between the polymer phases. If the PCL particle size is reduced the transfer of impurities is even more enhanced. In fact in PLA/PCL/MMT30B-g-P(LLA-co-CL) 80/20/5, which present the smallest PCL particles, shows the highest reduction of the PLA cold crystallization temperature.

In all the blends, during the second heating scan PLA presents double melting peak. The double melting endotherm of PLA is usually assigned to a melting-recrystallization phenomenon during the heating scan, due to unstable defective crystals [46].

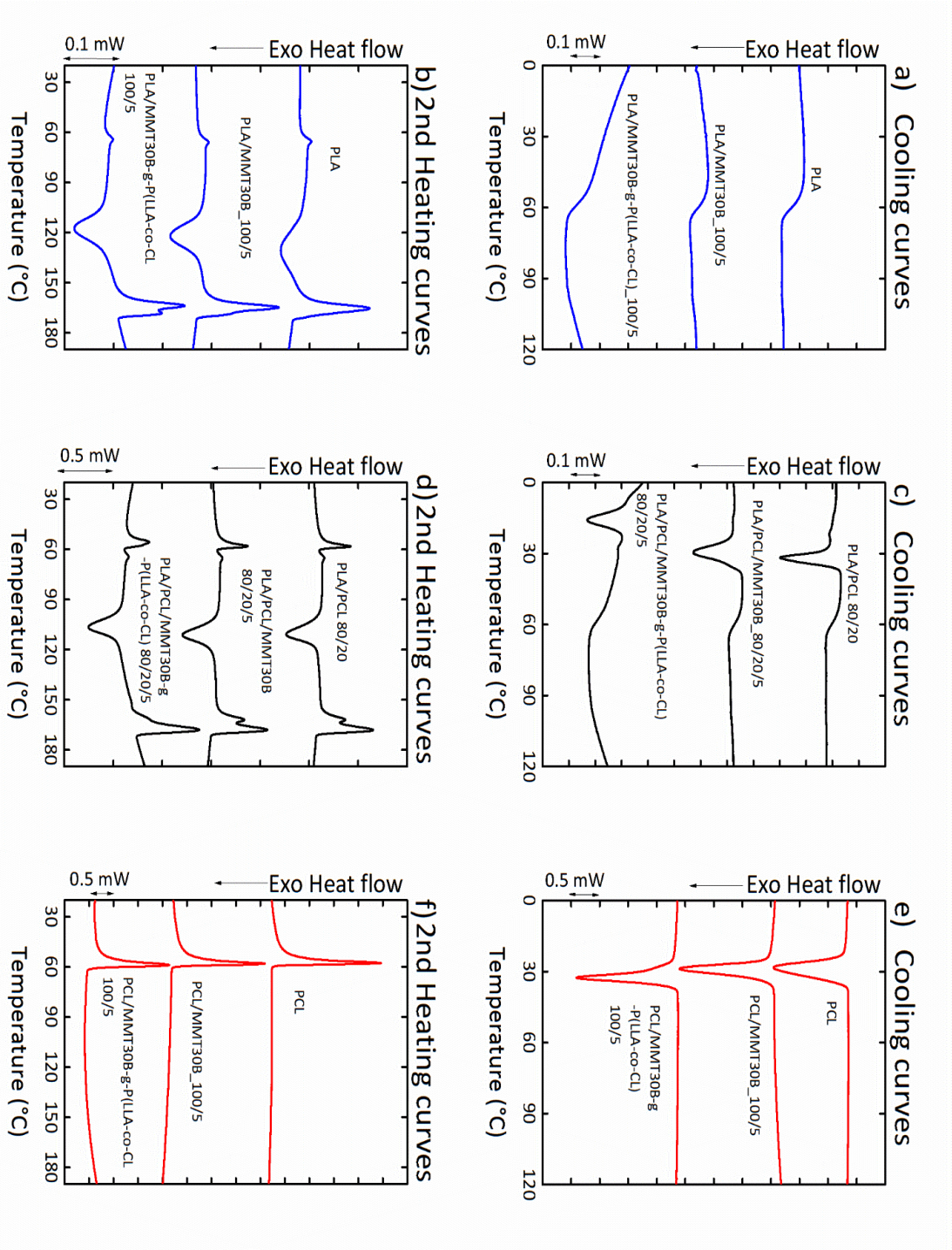

Figure 3.8 a) c) and e) cooling curves divided as reported inside the images and b) d) and f) second heating curves divided as reported inside the images.

Table 3.5 DSC data obtained analyzing cooling and 2nd heating curves on neat PLA, PLA/PCL_80/20 and neat PCL blends

	Cooling				2nd Heating			
	PCL Cryst.		PCL Melting		PLA Cold Cryst.		PLA Melting	
Sample	Tc (°C)	ΔHc (J/g)	Tm (°C)	ΔHm (J/g)	Tcc (°C)	ΔHcc (J/g)	Tm (°C)	ΔHm (J/g)
PLA	-	-	-	-	129.1	-27.8	165.6	33.3
PLA/MMT30B 100/5	-	-	-	-	122.1	-38.2	164.9	36.4
PLA/MMT30B-g-P(LLA-co-CL) 100/5	-	-	-	-	117.6	-31.5	163.8/168.1	25.0/8.9
PLA/PCL 80/20	21.7/31.8	-2.6/-45.0	58.2	45.0	110.8	-27.9	162.4/167.8	15.6/16.6
PLA/PCL/MMT30B 80/20/5	15.1/29.8	-4.5/-43.4	58.1	36.5	111.5	-31.9	162.0/168.1	15.1/19.8
PLA/PCL/MMT30-g-P(LLA-co-CL) 80/20/5	15.8/27.6	-36.7/-1.0	55.9	40.3	106.5	-28.2	167.5	31.5
PCL	28.4	-59.5	54.9	61.2	-	-	-	-
PCL/MMT30B 100/5	32.6	-56.8	58.0	63.1	-	-	-	-
PCL/MMT30B-g-P(LA-co-CL) 100/5	28.8	-59.2	57.8	55.4	-	-	-	-

3.6 Overall isothermal crystallization rate

The isothermal DSC experiments were performed following closely the procedure recommended by Lorenzo *et* al.[47]. The samples were first heated to 200 ºC and kept at that temperature for 3 min to erase their thermal history. Then they were cooled at a controlled rate of 60 ºC/min to the chosen isothermal crystallization temperatures (T_c). The isothermal crystallization temperature range was determined by preliminary tests to ensure that no crystallization occurred during the cooling step (see ref. 13).

In order to avoid degradation reactions, each sample was dried overnight at 60 ºC under vacuum before DSC measurements, and it was not used for more than two isothermal experiments. The inverse of the half-crystallization time, determined by isothermal crystallization from the melt employing DSC, provides an experimental measure of the overall crystallization rate, which includes both nucleation and spherulitic growth.

Figure 3.9 (the values of the data analyzed are reported in the experimental section) a) shows the overall crystallization rate (expressed as the inverse of half-crystallization time) as a function of the temperature for neat PLA, PLA/MMT30B 100/5 and PLA/MMT30B-g-P(LLA-co-CL) 100/5, while Figure 3.9 b) shows the same data for PLA/PCL 80/20, PLA/PCL/MMT30B 80/20/5 and PLA/PCL/MMT30B-g-P(LLA-co-CL) 80/20/5.

The solid lines correspond to the mathematical fits to the Lauritzen and Hoffman theory, explained in the experimental section of this work. All the samples display the typical *bell-shape* trend as well as theoretical values represented by the continue lines.

Neat PLA contains predominantly L stereo-isomer units, typically more than 96%, and a minor proportion of D units which act as defects to hinder the crystallization of L segments within the chains. The quantity of D-isomer lactide vary between 1,2%-1.6%.

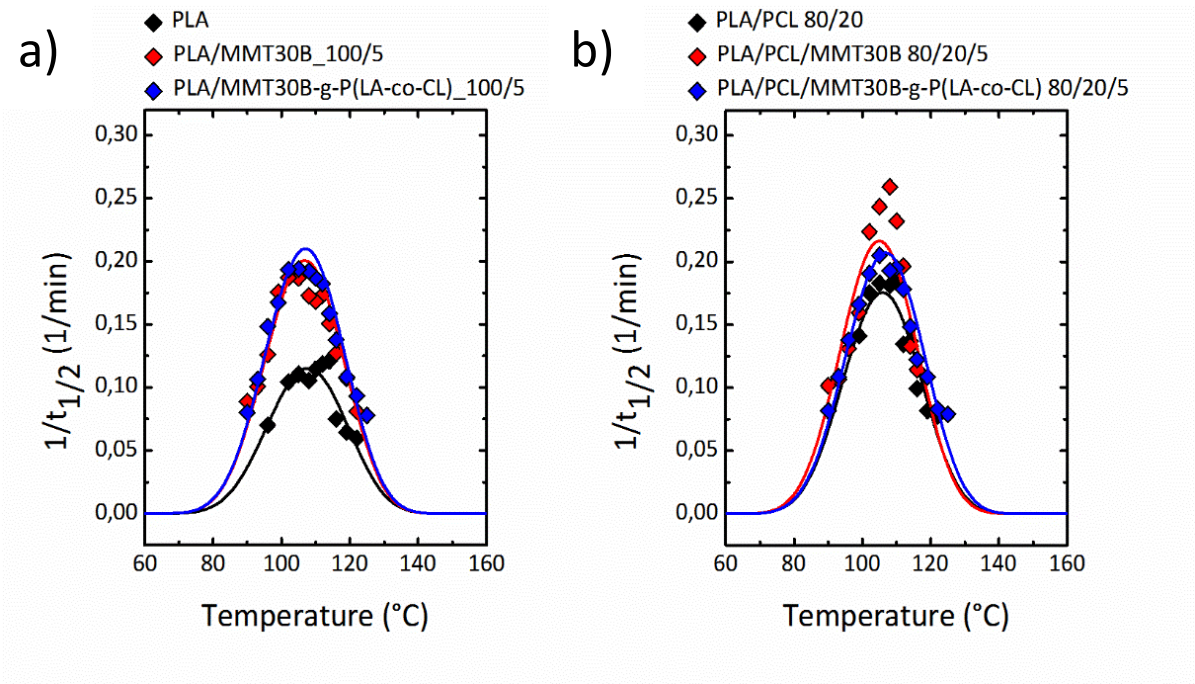

Figure 3.9 a) plots of $1/\tau_{1/2}$ as a function of Tc for neat PLA, PLA/MMT30B 100/5 and PLA/MMMT30B-g-P(LLA-co-CL) 100/5 and b) plots of $1/\tau_{1/2}$ as a function of Tc for PLA/PCL 80/20, PLA/PCL/MMT30B 80/20/5 and PLA/PCL/MMMT30B-g-P(LLA-co-CL) 80/20/5.

Experimental data shown in Figure 3.9 indicate that the crystallization rate of PLA is increased upon the addition of the organoclay based nanofillers. Both PLA/MMT30B 100/5 and PLA/MMT30B-g-P(LLA-co-CL) 100/5 show a crystallization rate two times higher than neat PLA. This enhancement effect is strictly connected to the introduction of active heterogeneities, that could improve the crystallization, upon the addition of the nanofillers.

The addition of PCL to PLA enhances the PLA crystallization rate, as suggested by non-isothermal experiments. Since PLA and PCL are immiscible, the interface of the phase-separated domains may provide favorable nucleation sites for PLA crystallization [48].

The addition of the organoclay based nanofillers does not change the results, since the increase resulting from the blending could cover any effect of the nanofiller.

The isothermal crystallization data obtained by DSC were analysed using the Avrami equation. The fits to the Avrami equation were performed using the Origin® plug in, developed by Lorenzo et al [49]. The procedure employed and examples of the results are presented in the experimental part.

Figure 3.10 displays that the Avrami index values (*n*) for the isothermal crystallization of PLA or the PLA phase within all prepared blends is included between 2 and 3 for most cases (although in some cases values closer to 2 were obtained). A values of 2 corresponds to bidimensional spherulites while 3 is predicted for instantaneously nucleated spherulites [50].

In neat PLA, as T_c increases, the Avrami index tends to increase. This is a typical trend, since nucleation becomes more sporadic as temperature increases. No other specific trends or differences between the different blends were observed.

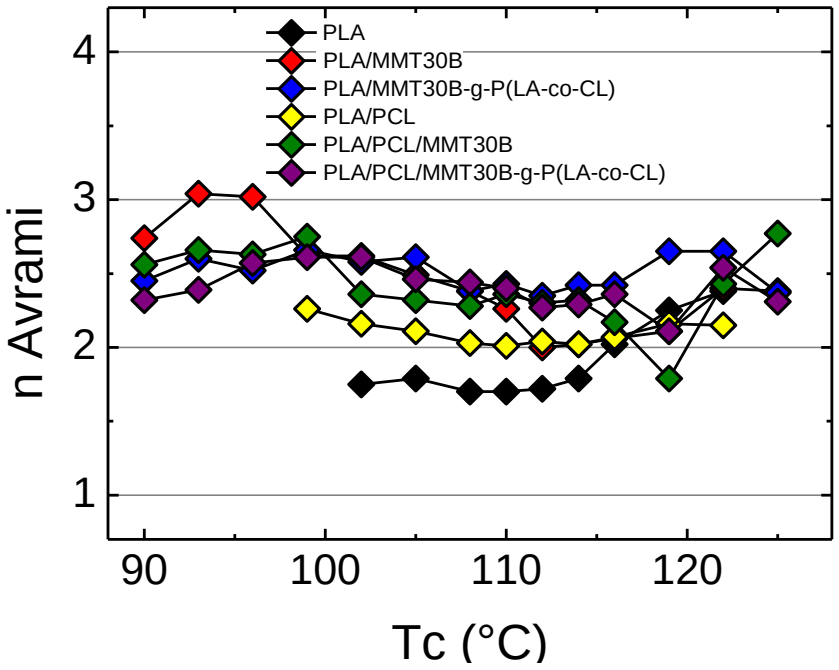

Figure 3.10 Avrami index of all the blends studied in relation with the Isothermal Crystallization Temperature (Tc)

4 CONCLUSIONS

Experimental techniques were employed to characterize MMT30B-g-P(LLA-co-CL) synthetized and to study the overall crystallization rate of PLA in blends composed by neat PLA and PLA/PCL both with and without the synthesized nanofiller and neat montmorillonite.

Talking about the synthesis of the grafted copolymer on the organoclay we can conclude that:

1. Nuclear magnetic resonance (^{1}H-NMR) analysis demonstrated that the ideal composition of the grafted copolymer, to enhance the interaction with the polymeric matrix (50% of lactide and 50% of ε-caprolactone), could be reached performing bulk reaction or using xylene as a solvent, while the reaction performed in toluene, at 85°C, is reacher in lactide.
2. Attenuated total reflection infrared analysis (ATR-IR) confirmed the successful grafting performing reactions in solvent, while bulk reaction present low grafting density.
3. Thermogravimetric analysis (TGA) demonstrated that conducting the grafting process in xylene there is the major percentage of grafted copolymer on MMT30B.

Considering all the information listed before it was decided to scale up the reaction conducted in xylene to obtain the amount of product needed for the subsequent analysis.

Analyzing the results obtained on neat PLA and PLA/PCL 80/20 blends with nanofillers we can state that:

1. Scanning electron microscopy (SEM) show that neat MMT30B is aggregated in larger particles than MMT30B-g-P(LLA-co-CL) because the second one is better exfoliated than the first one. Anyway both the nanofillers are immiscible in the PLA matrix. Considering PLA/PCL 80/20 blends, we can observe that these two polymers are immiscible as demonstrated by the *sea-island* morphology and that neat MMT30B doesn't have any compatibilizing effect, while MMT30B-g-P(LLA-co-CL) improve the interaction between the PLA and PCL phases, reducing the PCL particles size thanks to the copolymer grafted chains resulting in a better dispersion of the filler in the matrix.
2. TGA displayed that blends containing nanofillers present a lower thermal stability than blends without nanofillers. This because blends containing MMT30B were sonicated for 60 minutes and this procedure could lead to chain break of both PLA and PCL reducing molecular weight and thermal stability of the blends. Furthermore MMT30B can act as a catalyst in polyesters degradation, since the silicate layers surface of the clay are strongly acidic proton sites. MMT30B-g-P(LLA-co-CL) further increases the degradation of the blends. It is possible that the presence of LiCl traces could act as a pyrolysis catalyst

reducing thermal stability of blends. Furthermore the grafted copolymer chains, having a low molecular weight, could induce the degradation of the higher molecular weight neat polymer

3. non-isothermal Differential Scanning Calorimetry (DSC) on blends shows that PCL crystallization in PLA/PCL/MMT30B-g-P(LLA-co-CL) 80/20/5 is fractionated. PLA/PCL 80/20 and PLA/PCL/MMT30B 80/20/5 do not exhibit fractionated crystallization. PLA does not crystallize during cooling at the scanning rate employed (10 ºC/min) in no one of the samples because of the presence of 1.2% of D-isomer in the PLA matrix. During the second heating scan PLA is able to develop a cold crystallization peak in every samples. However, in neat PLA the peak is higher in temperature than in the other blends; this means that blending PLA with PCL promotes the cold crystallization. PLA/PCL/MMT30B-g-P(LLA-co-CL) 80/20/5 has the smallest PCL particles and the highest reduction of the PLA cold crystallization temperature. In all the blends, during the second heating scan PLA presents double melting peak.
4. isothermal DSC analysis demonstrate that the crystallization rate of PLA is increased upon the addition of the organoclay based nanofillers with respect to the one of neat PLA. Both PLA/MMT30B 100/5 and PLA/MMT30B-g-P(LLA-co-CL) 100/5 show a crystallization rate two times higher than neat PLA. The addition of PCL to PLA enhances the PLA crystallization. The addition of the organoclay based nanofillers in PLA/PCL blends does not change the rate of crystallization, since the increase resulting from the blending could cover any effect of the nanofiller.

5 EXPERIMENTAL SECTION

5.1 Materials

Montmorillonite30B (Sigma Aldrich) was dried in an oven at least for 24 hours. L-lactide (Sigma-Aldrich, CAS Number: 4511-42-6) was previously purified by recrystallization from boiling toluene followed by complete elimination of the solvent under vacuum for 3 hours. ε-caprolactone (Sigma-Aldrich, CAS Number: 502-44-3) was purified under vacuum distillation. Tin(II)octoate (Sigma-Aldrich-CAS Number: 301-10-0) was used as received . A mixture of xylene isomers (Sigma-Aldrich, CAS Number: 1330-20-7), previously dried on sodium sulfate, was used as solvent. Toluene (Sigma-Aldrich, CAS Number:108-88-3) was purified by distillation on sodium , and used as solvent. Poly(ε-caprolactone) (Mw = 80000 g/mol) was supplied by Solvay, poly(L-lactide) was supplied by Nature Works (Mw = 200000 g/mol 4032D, 1.2 % - 1.6 % D-isomer lactide). All glassware was dried in an oven at 105 °C at least 4 for hours.

5.2 Synthesis of the random copolymer lactide and ε-caprolactone grafted on montmorillonite

5.2.1 Bulk reaction

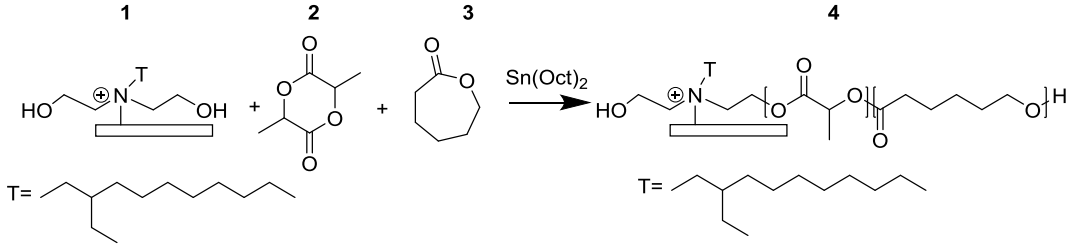

Figure 5.1 Synthesis of the MMT30B-g-P(LA-ran-CL) (4) starting from MMT30B (1), D,L-lactide (2) and ε-caprolactone (3).

In a flask equipped with three necks containing a magnetic stirrer and connected to the condenser with a Calcium Chloride ($CaCl_2$) septum at the head, are sequentially placed under nitrogen flow: MMT30B, D,L-lactide and ε-caprolactone. Tin(II) octoate ($Sn(Oct)_2$) is added after complete dissolution of the previous reactants. The quantity utilized are reported in Results and Discussion chapter.

The flask is stirred in an oil bath at a controlled temperature of 120°C for 48 hours. At the end of the reaction, the flask is cooled in an ice bath and after that, a small amount of dichloromehane is

added to reduce viscosity. In this solution is added an equal volume of aqueous solution of lithium chloride (LiCl) (1% wt) and the mixture is treated for 48h.

The two phases formed after this treatement are separated.

The aqueous phase should contain the clay which has not reacted, therefore, after filtering the clay and drying it in an oven at 100°C for 48 hours its weigh is registered.

The organic phase (DCM) is centrifuged for 30 minutes at 3000 rpm to separate the insoluble grafted polymer from the not-grafted (supernatant). The grafted polymer was placed in a vial and the residual solvent was eliminated under vacuum. The not-grafted polymer was precipitated from the supernatant using a 5-fold volume excess of methanol as non solvent, thus purify the polymer from the presence of monomers or oligomers with low molecular weight. The precipitate is placed in a separate vial and the residual solvent was removed under vacuum.

5.2.2 Solution reactions

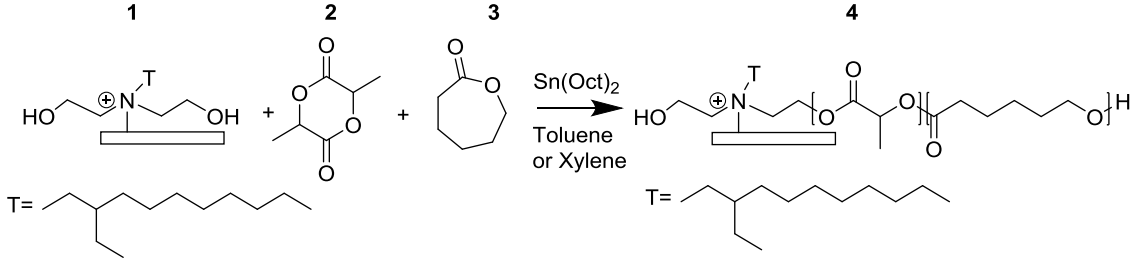

Figure 5.2 Synthesis of the MMT30B-g-P(LA-ran-CL) (4) starting from MMT30B (1), D,L-lactide (2) and ε-caprolactone (3) in presence of a solvent (toluene or xylene).

In a Schlenk tube equipped with a magnetic stirrer, under nitrogen flow, are sequentially placed: montmorillonite, D,L-lactide, ε-caprolactone and the solvent. Tin(II) octoate ($Sn(Oct)_2$) is added only after complete dissolution of the previous reactants in the solvent. The Schlenk tube is stirred in an oil bath at a controlled temperature (85°C if the solvent is toluene and 120°C if it is xylene), ensuring that the stirring is always effective. The reaction is conducted for 24 hours.

At the end of the reaction, the Schlenk tube is cooled in an ice bath and after that a small amount of dichloromehane is added to reduce viscosity. At this solution is added an equal volume of aqueous solution of lithium chloride (LiCl) (5% wt) and the mixture is treated for 48h.

The aqueous phase should contain the clay which has not reacted, therefore, after filtering the clay and drying it in an oven (48 hours) it was weighted.

The organic phase (DCM) is centrifuged for 60 minutes at 3000 rpm to separate the insoluble grafted polymer from the not-grafted (supernatant). The grafted polymer was placed in a vial and the residual solvent was eliminated under vacuum. The not-grafted polymer was precipitated from

the supernatant using a 5-fold volume excess of hexane as non solvent, thus cleaning the polymer from the presence of monomers or oligomers with low molecular weight. The precipitate was placed in a separate vial and the residual solvent was removed under vacuum.

In Table 5.1 details about different preparations are reported.

Table 5.1 Initial data of the reactions

Sample	Procedure				
	MMT30B (w/w %)	**Cat. (mol/mol %)**	**Time (h)**	**Temp. (°C)**	**Solvent**
MMT30BCLLA50501	1.9	0.2	48	120	-
MMT30BCLLA50502	1.0	0.1	48	120	-
MMT30BCLLA50503	1.0	0.1	48	120	-
MMT30BCLLA50504	1.0	0.1	24	120	-
MMT30BCLLA50505	1.0	0.1	24	85	Toluene
MMT30BCLLA50506	1.9	0.2	24	85	Toluene
MMT30BCLLA50507	3.8	0.5	24	85	Toluene
MMT30BCLLA50508	1.0	0.1	24	120	Xylene
MMT30BCLLA50509	1.9	0.2	24	120	Xylene

5.3 Preparation of the PLA/PCL Blends

Three different kind of blends were used in this work:

- PLA/PCL;
- PLA/PCL/MMT30B;
- PLA/PCL/MMT30B-g-P(LLA-co-CL).

Every blend was prepared following the subsequent procedure.

Neat PLA, neat PCL and the eventual nanofiller were weighed (each mass is reported in Table 5.2) and put in a 100 mL flask.

Dichlomethane was added to obtain a solution with a polymer concentration of 1g/dL.

Part of the solvent has been evaporated at 25°C and the solution was sonicated for 60 minutes to obtain a better homogenization of the components.

The solution obtained was left at room temperature for 24 hours and afterwards put in a vacuum oven at 60°C for 24 hours to completely remove the solvent.

Table 5.2 Weight composition of PLA/PCL blends

Blend	PLA (mg)	PCL (mg)	Nanofiller (mg)
PLA	1000	0	50
80/20	800	200	50
PCL	0	1000	50

5.4 Characterization of the MMT30B-g-P(LLA-co-CL) copolymer

The synthesized compounds were characterized using different laboratory techniques:

- Nuclear magnetic resonance (^{1}H-NMR)

  The ^{1}H-NMR spectra were recorded in $CDCl_3$ using a spectrometer Varian "Mercury 400" operating at 400 MHz. Chemical shift (δ) for ^{1}H are given in ppm relative to the known signal of the internal reference (TMS).

  ^{1}H-NMR analysis of the copolymers:

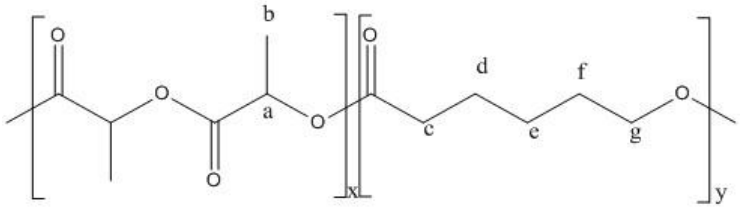

Figure 5.3 Structure of random copolymer lactide and ε-caprolactone P(LLA-co-CL).

1 H of CH (a) at 5.12 ppm

3 H of CH_3 (b) at 1.37 ppm

2 H of CH_2 (c) at 4.08 ppm

6 H of CH_2 (d, e, f) at 1.61 ppm

2 H of CH_2 (g) at 2.34 ppm

- Attenuated total reflection infrared spectroscopy (ATR-IR)

  ATR-IR spectroscopy was used to characterize the grafted polymer**.**

  The infrared spectra were recorded using ALPHA FT-IR Spectrometer of Bruker in a range between 4000 cm^{-1} and 400 cm^{-1}. The spectra obtained is reported in Results and discussion chapter.

- TGA analysis

  The weight percentage of grafted copolymers as a function of temperature was determined using a thermobalance TA Instruments, model Q500, consisting in an electronic microbalance placed inside an oven. The system that control the temperature of the oven is connected to a computer which records the weight loss of the sample related to the temperature. For every analysis about 5-10 mg of sample were weighed.

  Measurements were conducted under nitrogen atmosphere from 40°C to 600°C using a heating rate of 20°C/min.

5.5 Characterization of the Blends

- TGA analysis

  The weight percentage of grafted copolymers and blends as a function of temperature was determined using a thermobalance TA Instruments, model Q500. For every analysis about 5-10 mg for each sample were weighed.

  Measurements were conducted under nitrogen atmosphere from 40°C to 600°C using a heating rate modulated by the first derivative of the loss in mass.

- SEM analysis

  Prior to microscopic observation, the samples were cut under liquid nitrogen to create a plane face. The surface of the sample was held at approximately -150 °C to reduce the degree of surface deformation. The samples were then coated with gold and observed under a Zeiss EP EVO 50 scanning electron microscope operating at a working voltage of 20 kV.

- DSC analysis

  For the thermal characterization of the copolymers and blends a differential scanning calorimeter Perkin Elmer DSC 8500 has been used, equipped with a cooling system INTRACOOLER II with a nitrogen flow of 20 ml/min. Heating scans were performed in an inert atmosphere using high purity nitrogen. The thermal and enthalpy calibration was performed with an indium sample (Tm = 156.6°C and ΔHm = 28.71 J/g). About 5 mg for each sample have been weighed. Two different analysis were performed on the sample: dynamic and isothermal scans.

  The dynamic scans of all blends, PLA/PCL, PLA/PCL/MMT30B and PLA/PCL/MMT30B-g-P(LLA-co-CL) were performed according to the following steps:

  - Heating from 25°C to 200°C at 10°C/min;
  - 3 minutes at this temperature;
  - Cooling from 200°C to -20°C at 10°C/min;
  - 3 minutes at this temperature;
  - Heating from -20°C to 200°C at 10°C/min.

  Apart from PLA, isothermal DSC analysis were performed on the following blends: PLA/MMT30B 100/5, PLA/PCL/MMT30B-g-P(LLA-co-CL) 100/5, PLA/PCL 80/20, PLA/PCL/MMT30B 80/20/5 and PLA/PCL/MMT30B-g- P(LLA-co-CL) 80/20/5.

  The steps performed for isothermal analysis were the following:

  - Heating from 25°C to 200°C at 20°C/min;

- 3 minutes at this temperature;
- Cooling form 200°C to the isothermal crystallization temperature (Tc) at 60°C/min;
- Keep at this temperature for 30 min (this time is estimated as three times the time necessary to develop 50% of the crystals);
- Heating from Tc to 200°C at 10°C/min.

Different values of Tc have been taken; this values were: 140°C, 136°C, 132°C, 128°C, 125°C, 122°C, 119°C, 116°C, 114°C, 112°C, 110°C, 108°C, 105°C, 102°C, 99°C, 96°C, 93°C, 90°C.
Each sample pan was replaced after two isothermal analyses because the samples suffers from degradation when they are subjected at too many scans.
The range in which to work was selected knowing that the crystallization process could happen in a temperature range that starts from 30°C over the Tg and ends 10°C before the melting of the considered polymer. In our study the range for PLA resulted of 50°C.
In Figure 5.4 is shown an example of DSC scans, as a function of time, collected at different crystallization temperature in isothermal conditions starting from the melt state.

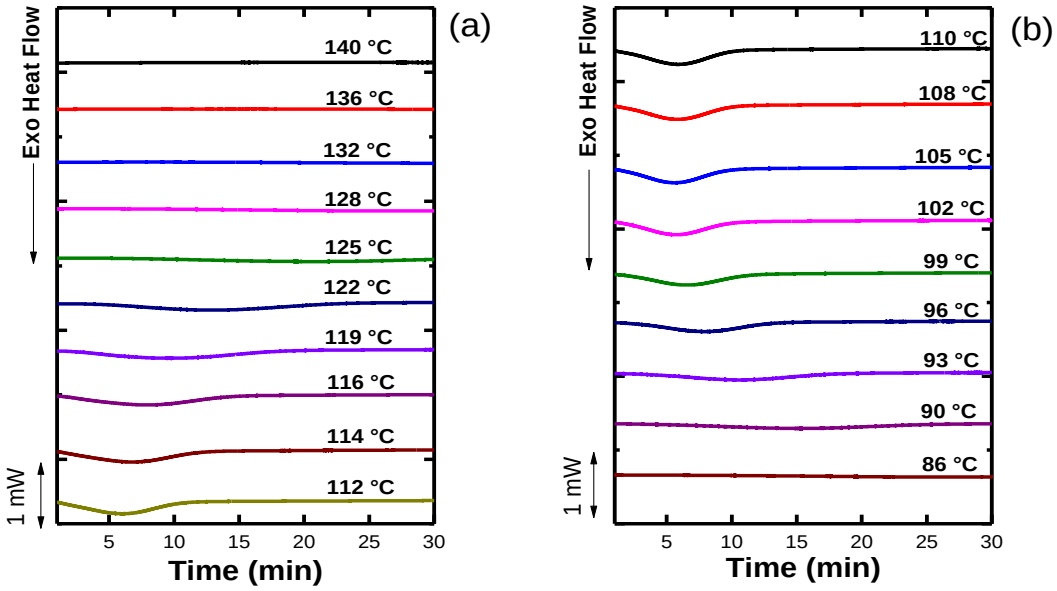

Figure 5.4 Isothermal scans for PLA/MMT30B-g-P(LLA-coCL)

The isothermal scans show information on crystallization rate of PLA. For all scans the half-crystallization time ($\tau_{50\%}$) has been calculated. This time represents how long does the sample takes to reach 50% relative conversion to semi-crystalline state. The inverse overall crystallization rate is proportional to the half-crystallization time (as reported in Results and Discussion chapter).

To analyze the data obtained from DSC in isothermal conditions we used the Avrami's equation. The application of this method was possible because every blend shows, in intermediate isotherm conditions, a considerable increase in crystallization rate.
According to Avrami, the progress of the isothermal crystallization can be expressed by the equation[47]:

$1-V_c = \exp[-k(t-t_0)^n]$ Equation 5.1

Where *Vc* is the crystalline volume fraction, *k* is the constant rate of the overall crystallization, t_0 is the induction time, *n* is the Avrami index that assumes different values depending on the type of geometry of crystal growth and the type of nucleation. Applying the logarithmic properties on both sides of the equation 5.1, the following equation can be obtained:

$$\log [-\ln (1 - Vc)] = \log (k) + nlog(t - t_0) \quad \text{Equation 5.2}$$

This equation is called Avrami linear equation.
Plotting $\log [-\ln (1 - Vc)]$ as a function of $\log (t - t_0)$ the values of *k* and *n* can be obtained.
A very important value in the Avrami's theory is the time required by the material to reach the half-crystallization time indicated as $\tau_{1/2}$ or $\tau_{50\%}$. It is possible to calculate it through this equation[47]:

$$\tau_{1/2} = \left(\frac{-\ln (1-Vc)}{k}\right)^{1/n} = \left(\frac{-\ln (0.5)}{k}\right)^{1/n} \quad \text{Equation 5.3}$$

Conversion of the semicrystalline state from 3% to 20% was used for all the samples; the conversion values lower than 3% fall within equipment errors, while those exceeding 20% have shown a deviation between the theoretical and the experimental data[49].

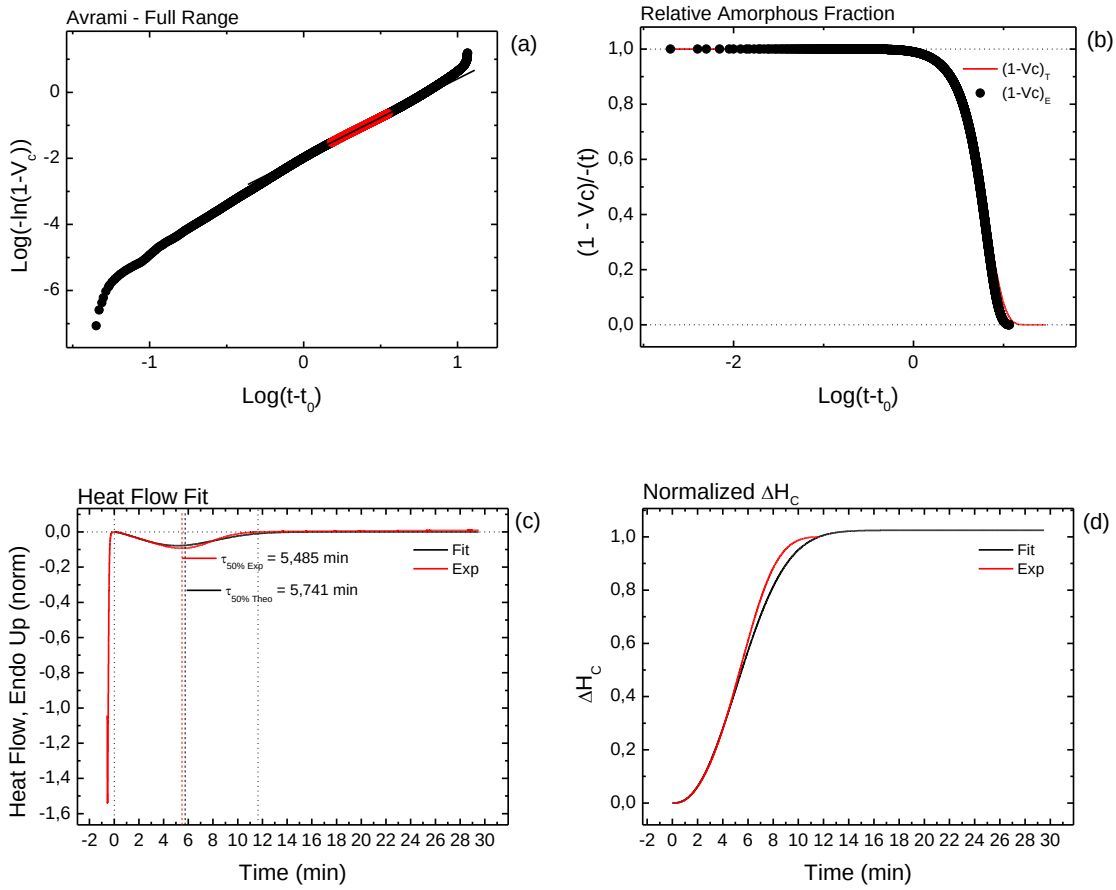

Figure 5.4 a) Avrami plot. b) Unconverted relative volumetric fraction as a function of time for the isothermal crystallization of the neat PLA at 112°C. Comparison between the experimental data and Avrami fit. c) Comparison between experimental DSC isothermal and Avrami prediction for PLA isothermally crystallized. d) Change of crystallization enthalpy as a function of crystallization time

In Table 5.3 are listed all the data obtained applying the Avrami model on our blends. Tc is the isotherm temperature, n is the Avrami index, K^{-n} is the constant of overall crystallization, both the $\tau_{1/2}$ represent the time required to join 50% conversion to the crystalline state and R^2 is the linearity error. These data are very important because they are needed to compare the crystallization rate of different blends.

Table 5.3 Data obtained from the Avrami model

Sample	Tc (°C)	n	$K^{-n}(min^{-n})$	τ1/2 Theo (min)	τ1/2 Exp (min)	R^2
	122	2.38	0.0007	17.602	16.767	1
	119	2.25	0.0013	16.051	15.492	1
	116	2.02	0.0032	14.44	13.335	1
PLA	114	1.79	0.0109	10.125	8.788	0.9996
	112	1.72	0.0135	9.839	8.43	0.9996
	110	1.7	0.0132	10.26	8.727	0.9995
	108	1.7	0.0116	11.075	9.475	0.9995

	105	1.79	0.0103	10.514	9.05	0.9991
	102	1.75	0.0102	11.208	9.582	0.9991
PLA/MMT30B_100/5	125	2.38	0.00149	13.278	12.855	1
	122	2.4	0.00181	11.935	12.34	0.9999
	119	2.11	0.00643	9.196	9.318	0.9997
	116	2.06	0.00909	8.159	7.863	0.9995
	114	2.02	0.0125	7.268	6.642	0.9999
	112	2	0.0162	6.538	5.767	0.9996
	110	2.26	0.00996	6.535	5.937	0.9994
	108	2.38	0.00875	6.299	5.789	0.9992
	105	2.49	0.00896	5.745	5.352	0.9995
	102	2.62	0.00739	5.672	5.345	0.9995
	99	2.62	0.00608	6.09	5.696	0.9993
	96	3.02	0.00116	8.303	7.94	0.9996
	93	3.04	0.000551	10.428	9.933	0.9994
	90	2.74	0.000822	11.732	11.254	0.9998
PLA/MMT30B-g-P(LLA-co-CL)_100/5	125	2.37	0.00149	13.4	12.85	0.9999
	122	2.65	0.00124	10.777	10.727	1
	119	2.65	0.00203	9.035	9.238	0.9999
	116	2.42	0.00568	7.29	7.252	0.9999
	114	2.42	0.0076	6.436	6.304	0.9999
	112	2.35	0.0114	5.741	5.485	1
	110	2.43	0.00972	5.782	5.357	0.9995
	108	2.38	0.0113	5.622	5.205	0.9994
	105	2.61	0.0086	5.39	5.154	0.9998
	102	2.58	0.00896	5.41	5.165	0.9998
	99	2.66	0.00535	6.23	5.972	0.9998
	96	2.52	0.00482	7.201	6.737	0.9994
	93	2.6	0.00176	9.959	9.389	0.9997
	90	2.45	0.00119	13.418	12.503	0.9995
PLA/PCL_80/20	122	2.15	0.00285	12.931	12.874	1
	119	2.16	0.00312	12.134	12.232	0.9997
	116	2.07	0.00513	10.702	10.07	1
	114	2.02	0.00975	8.269	7.302	0.9991
	112	2.04	0.00901	8.365	7.426	0.9992
	110	2.01	0.0202	5.794	5.435	0.9999
	108	2.03	0.0189	5.87	5.515	1
	105	2.11	0.0175	5.703	5.467	1
	102	2.16	0.0148	5.919	5.71	1
	99	2.26	0.0079	7.264	7.082	1
	125	2.77	0.000464	13.991	14.482	0.9995
	122	2.43	0.00159	12.152	13.025	0.9998
	119	2.79	0.00897	11.378	11.625	0.9993
	116	2.17	0.00567	9.17	8.735	1
	114	2.32	0.00578	7.889	7.526	0.9998

PLA/PCL/MMT30B_80/20/5	112	2.3	0.0139	5.5	5.094	0.9994
	110	2.36	0.0194	4.537	4.31	0.9998
	108	2.28	0.0291	4.021	3.858	0.9999
	105	2.32	0.0232	4.317	4.108	0.9997
	102	2.36	0.0176	4.73	4.472	0.9996
	99	2.75	0.00404	6.517	6.275	0.9998
	96	2.63	0.00284	8.1	7.628	0.9992
	93	2.66	0.00161	9.76	9.372	0.9998
	90	2.56	0.00182	10.207	9.829	0.9999
PLA/PCL/MMT30B-g-P(LLA-co-CL)_80/20/5	125	2.31	0.0018	13.195	12.64	0.9998
	122	2.54	0.00121	12.147	12.035	1
	119	2.11	0.00573	9.667	9.2	1
	116	2.36	0.00428	8.613	8.183	1
	114	2.29	0.00725	7.336	6.738	0.9997
	112	2.27	0.011	6.191	5.61	0.9991
	110	2.4	0.0113	5.573	5.122	0.9992
	108	2.44	0.0103	5.589	5.187	0.9993
	105	2.46	0.012	5.206	4.879	0.9994
	102	2.61	0.00796	5.539	5.248	0.9996
	99	2.61	0.00558	6.353	6.017	0.9996
	96	2.57	0.00364	7.738	7.258	0.9992
	93	2.39	0.00281	10.034	9.203	0.999
	90	2.32	0.00175	13.156	12.237	0.9994

Avrami's index depends on the size of the crystals and on the type of nucleation that occurs in the system.

The constant of overall crystallization k^{-n} is expressed in $(min)^{-n}$ and depends on Avrami's index. In order to eliminate this dependence, k^{-n} has been normalized in k raising $1/n$, $(min^{-n})^{1/n}$.

Moreover the k^{-n} normalization allows us to avoid error in comparing the parameters. Figures 5.5 shows the variation of k values as a function of crystallization temperature. The trend of these parameters is related with the crystallization rate.

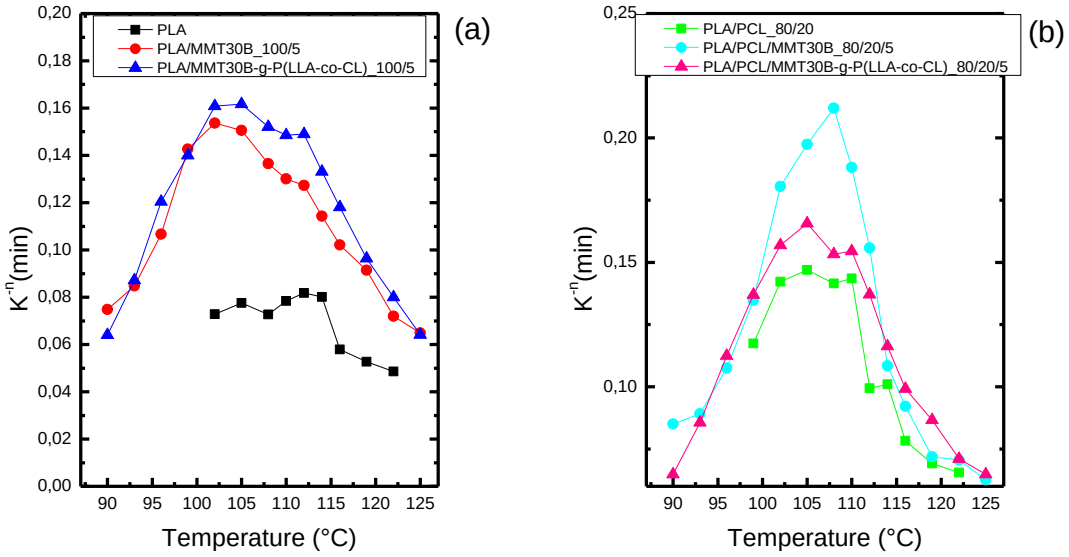

Figure 5.5 a) variation of k as a function of the temperature for neat PLA, PLA/MMT30B_100/5 and PLA/MMMT30B-g-P(LLA-co-CL)_100/5, b) variation of k as a function of the temperature for PLA/PCL_80/20, PLA/PCL/MMT30B_80/20/5 and PLA/PCL/MMMT30B-g-P(LLA-co-CL)_80/20/5

After the application of the Avrami's equation, the theory of Lauritzen and Hoffman was used to determine parameters such as the energy barrier for growth and nucleation (K^{τ}_{g}), the folding surface free energy (σ_e) and the work required to make a bend (q).

For the application of this model, we need to calculate the value of the temperature at the melting equilibrium (Tm^0) through the Hoffmann-Weeks method[51].

The Tm^0 is experimentally extrapolated by observing melting points in the heating scans of each sample.

Figure 5.6 a) and b) shows an example of heating scans, at 20 °C/min, performed after the isothermal crystallization. We can observe two melting peaks indicated by the arrows: one is the first melting temperature (Tm_1) and the other is the second melting temperature (Tm_2). Plotting Tm_2 vs Tc and Tm = Tc, the value of Tm_0 was obtained from the point of intersection of the lines obtained as shown in Figure 5.6 c).

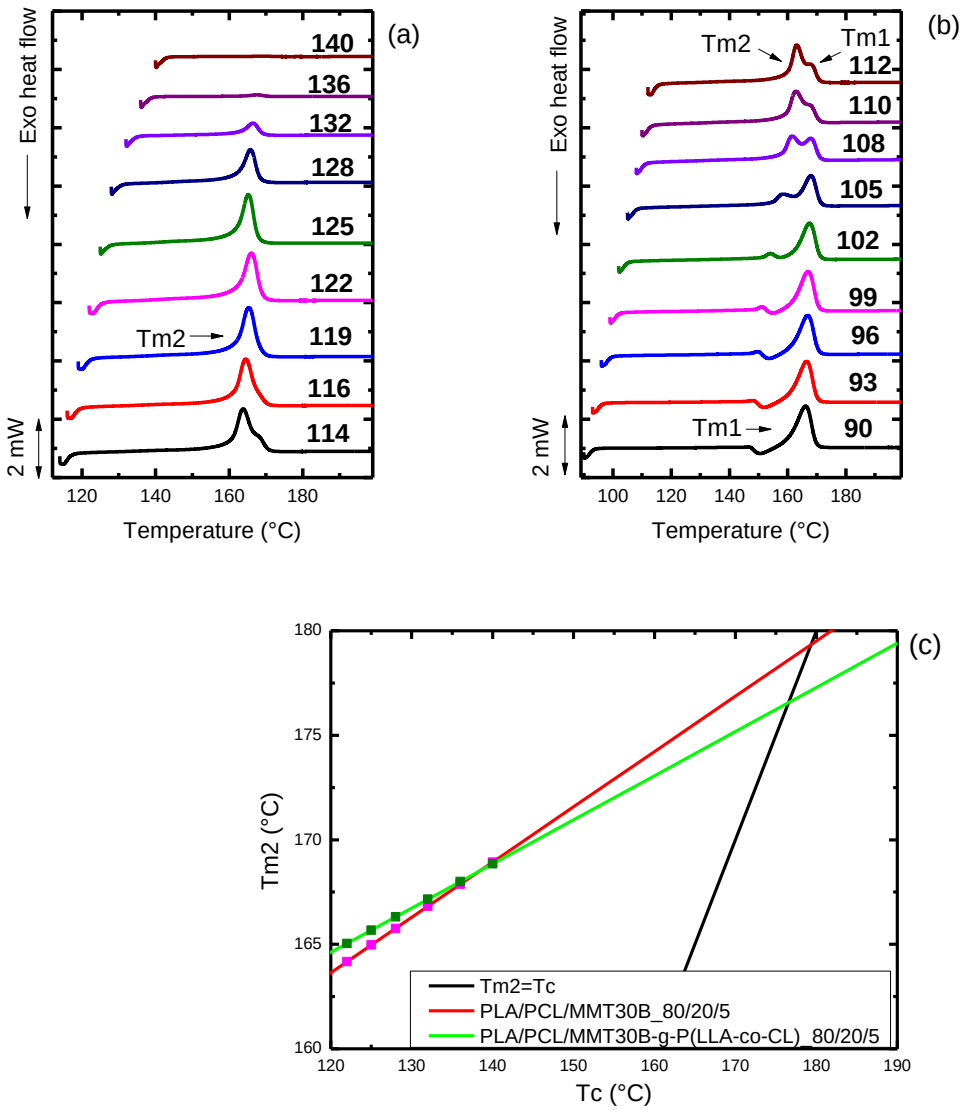

Figure 5.6 a) and b) heating scan at 20°C/min after isothermal crystallization of PLA/PCL/MMT30B_80/20/5, c) variation of Tm2 with Tc for PLA/PCL/MMT30B_80/20/5 and PLA/PCL/MMT30B-g-P(LLA-co-CL)_80/20/5

The Tm_0 values fall in the range of 176 -179°C.

Knowing the Tm_0 and the data of isothermal crystallization rate it is possible to apply the equation of Lauritzen-Hoffman in order to compare the variations between the experimental and theoretical data of the overall crystallization rate ($1/\tau_{1/2}$ vs Tc) and the closeness of the values obtained by the two methods.

The evaluation of the data obtained is fully reported in Result and Discussion Chapter.

Table 5.4 shows the values obtained in term of energy barrier of nucleation and growth crystal increase (K^{τ}_g), σ_e indicates the free energy of folding, σ is the lateral surface free energy, q the work necessary to achieve a bending, and R^2 is the linearity error.

Table 5.4 Data obtained using the L-H model with DSC

Sample	K^{τ}_{g} (II) (K^2)	σ (erg/cm^2)	σ_e (erg/cm^2)	q (erg)	R^2
PLA	2.99 E+05	8.08	259.34	9.57 E-13	0.9895
PLA/MMT30B 100/5	3.04 E+05	8.08	264.58	9.76 E-13	0.9899
PLA/MMT30B-g-P(LLA-co-CL) 100/5	3.01 E+05	8.08	261.97	9.67 E-13	0.9938
PLA/PCL 80/20	3.2 E+05	8.08	278.68	1.03 E-12	0.9894
PLA/PCL/MMT30B 80/20/5	3.17 E+05	8.08	276.86	1.02 E-12	0.9811
PLA/PCL/MMT30B-g-P(LLA-co-CL) 80/20/5	3.04 E+05	8.08	265.01	9.78 E-13	0.992

BIBLIOGRAPHY

[1] Yu Z., Yin J., Yan S., Xie Y., Ma J., Chen X.. Biodegradable poly(l-lactide)poly(ε-caprolactone)-modified montmorillonite nanocomposites Preparation and characterization. Polymer 48 (2007) 639-6447 .

[2] A. Casale, L'Acido Polilattico: dalla scoperta alle applicazioni attuali, Workshop tecnico-scientifico: "Opportunità applicative del PLA: Problematiche ed aspettative", Alessandria (TO), 2014

[3] Nair L., Laurencin C. Biodegradable polymers as biomaterial. Progress in Polymer Science 32 (2007) 762-798

[4] Tian H., Tang Z., Zhuang X., Chen X., Jing X. Biodegradable synthetic polymers Preparation , functionalization and biomedical application Progress in Polymer Science 37 (2012) 237-280 .

[5] Harris A., Lee E. Improving Mechanical Performance of Injection Molded PLA by Controlling Crystallinity Journal of Applied Polymer Science 107 (2008) 2246-2255 .

[6] Mano J., Gomez Ribelles J., Alves N., Salmeron Sanchez M. Glass transition dynamics and structural relaxation of PLLA studied by DSC: Influence of crystallinity Polymer 46 (2005) 8258-8265.

[7] Armentano I., Bitinis N., Fortunati E., Mattioli S., Rescignano N., Verdejo R., Lopez-Manchado M., Kenny J. Multifunctional nanostructured PLA materials for packaging and tissue engineering Progress in Polymer Science 38 (2013) 120-1747.

[8] Paul M., Alexandre M., Degee P., Calberg C., Jerome R., Dubois P. Exfoliated Polylactide/Clay Nanocomposites by In-Situ Coordination – Insertion Polymerization Macromolecular rapid Communication 24 (2003) 561-566.

[9] Chandra R., Rustgi R. Biodegradable polymers. Progress in Polymer Science 23 (1998) 1273-1335

[10] "Labet M., Thielemans W. Synthesis of polycaprolactone: a review Chemical Society Rewievs 38 (2009) 3484-3504.

[11] Khanna A., Sudha Y., Pillai S., Rath S. Molecular modeling studies of poly lactic acid initiation mechanisms Journal of Molecular Modeling 14 (2008) 367-374.

[12] Stridsberg K., Ryner M., Albertsson A. Controlled Ring-Opening Polymerization: Polymers with designed Macromolecular Architecture Springer 2002 41–65.

[13] Madhavan Nampoothiri K., Nair N., John R. An overview of the recent developments in polylactide (PLA) research Bioresource Technology 101 (2010) 8493-8501.

[14] Garlotta D. A Literature Review of Poly (Lactic Acid) Journal of Polymers and the Environment 9 (2001) 63-84.

[15] Inkinen S., Hakkarainen M., Albertsson A. Sodergard A. From Lactic Acid to Poly (lactic acid) (PLA): Characterization and Analysis of PLA and Its Precursors Biomacromolecules 12 (2011) 53-532.

[16] Triantafillidis C., Lebaron P., Pinnavaia T. Thermoset Epoxy- Clay Nanocomposites The Dual Role of Diamines as Clay Surface Modifiers and Polymer curing agents Journal of Solid State Chemistry 167 (2002) 354-362.

[17] Alexandre M., Dubois P. Polymer-layered silicate nanocomposites preparation , properties and uses of a new class of materials Materials Science and Engineering 28 (2000) 1-63.

[18] Salam H., Dong Y., Davies I. Development of biobased polymerclay nanocomposites: A critical rewiev - Fillers and Reinforcements for Advanced Nanocomposites (2015) 101- 134.

[19] Bourbigot S., Fontaine G., Bellayer S., Delobel R. Processing and nanodispersion: A quantitative approach for polylactide nanocompositePolymer Testing 27 (2008) 2-10.

[20] Reddy M., Vivekanandhan S., Misra M., Bhatia S., Mohanty A. Biobased plastics and bionanocomposites: Current status and future opportunities Progress in Polymer Science 38 (2013) 1653-1689.

[21] Ajellal et al. Metal-catalyzed immortal ring-opening polymerization of lactones, lactides and cyclic carbonates. - Dalton transactions 39 (2010) 8363-8376.
[22] Beaucage G., Stein R. Tacticity Effects on Polymer Blend Miscibility Flory-Huggins-Staverman Analysis Macromolecules 24 (1993) 1603-1608.
[23] Koning C., Duin M., Pagnoulle C., Jerome R. Strategies for compatibilization of polymer blends Progress in Polymer Science 23 (1998) 707-757.
[24] Dell'Erba R., Groeninckx G., Maglio G., Malinconico M., Migliozzi A. Immiscible polymer blends of semicrystalline biocompatible components Thermal properties and phase morphology analysis of PLLA/PCL blends Polymer 42 (2001) 7831-7840.
[25] Goffin A., Habibi Y., Raquez J., Dubois P. Polyester-Grafted Cellulose Nanowhiskers: A New Approach for Tuning the Microstructure of Immiscible Polyester blends Applied materials and interfaces 4 (2012) 3364-3371.
[26] Italian Association of Science and Technology of macromolecules (AIM), "Structural polymeric materials," Gargnano (Bs), 1989.
[27] Lorenzo A., Arnal M., Albuerne J., Muller A. DSC isothermal polymer crystallization kinetics measurements and the use of the Avrami equation to fit the data: guidelines to avoid common problems Polymer Testing 26 (2007) 222-231.
[28] Ehrenstein G., "Polymeric Materials: Structure," *Properties, Applications (Cincinnati: Hanser),* 2001.
[29] A. J. Muller, "Structure and properties of semi-crystalline polymers Venezuela Grupo de polimeros USB Universidad Simon Bolivar.
[30] Abe H., Kikkawa Y., Inoue Y., Doi Y. Morphological and kinetic analysis of regime transition for Poly[(S)-lactide] crystal growth Biomacromolecules 2 (2001) 1007-1014.
[31] U. W. Gedde, *Polymer Phisics*. Springer Science, 1995.
[32] Lo Re G., Benali S., Habibi Y., Raquez J., Dubois P. Stereocomplexed PLA nanocomposites: From in situ polymerization to materials properties European Polymer Journal 54 (2014) 138-150.
[33] "Lopez-Rodriguez N., Lopez-Arraiza A., Meaurio E., Sarasua J. Crystallization , Morphology , and Mechanical Behavior of Polylactide Poly (ε-caprolactone) Blends Polymer Engineering and Science 2006 1299-1309.
[34] "Pollet E., Delcourt C., Alexandre M., Dubois P. Organic-inorganic nanohybrids obtained by sequential copolymerization of ε-caprolactone and L,L-lactide from activated clay surface Macromolecular Chemistry and Phisics 205 (2004) 2235-2244.
[35] Peponi L., Marcos-Fernández A., Kenny J. Nanostructured morphology of a random P(DLLA-co-CL) copolymer Nanoscale research Letters 7 (2012) 103-110.
[36] Paul et al (Plasticized) polylactide(organo-)clay nanocomposites by in situ intercalative polymerization Macromolecular Chemistry and Phisics 206 (2005) 484-498.
[37] Failla S. Crystallization and morphology of the PLLA phase within random poly (L-lactide-ran-ε-caprolactone) 2013.
[38] Lepoittevin B., Pantousier N., Alexandre M., Calberg C., Jerome R., Dubois P. Polyester layered silicate nanohybrids by controlled grafting polymerization Journal of Materials Chemistry 182 (2003) 95-102.
[39] Mclauchlin A., Thomas N. Preparation and thermal characterisation of poly (lactic acid) nanocomposites prepared from organoclays based on amphoteric surfactant 94 (2009) 868-872.
[40] Wu D., Zhang Y., Zhang M., Zhou W. Phase behavior and its viscoelastic response of polylactide poly (e -caprolactone) blend 44 (2008) 2171-2183.
[41] Arnal M., Matos M., Morales R., Santana O., Muller A. Evaluation of the fractionated crystallization of dispersed polyolefins in a polystyrene matrix Macromolecular Chemistry and Phisics 199 (1998) 2275-2288.

[42] Yahiaoui F., Benhacine F., Ferfera-Harrar H., Habi A., Jadj-Hamou A., Grohens Y. Development of antimicrobial PCL nanoclay nanocomposite films with enhanced mechanical and water vapor barrier properties for packaging applications Polymer Bulletine 72 (2015) 235-254.
[43] Muller A., Avila M., Salazar J. Crystallization of PLA-based materials Science and Technology : Processing, Properties, Additives and Applications (2014) 66-98.
[44] Castillo R., Muller A., Raquez J., Dubois P. Crystallization Kinetics and Morphology of Biodegradable Double Crystalline PLLA- b -PCL Diblock Copolymers Macromolecules 43 (2010) 4149-4160.
[45] Cocca M., Di Lorenzo M., Malinconico M., Frezza V. Influence of crystal polymorphism on mechanical and barrier properties of poly (L -lactic acid) European Polymer Journal 47 (2011) 1073-1080.
[46] Stoclet G., Seguela R., Lefebvre J. Morphology , thermal behavior and mechanical properties of binary blends of compatible biosourced polymers: Polylactide/polyamide11 Polymer 52 (2011) 1417-1425.
[47] Lorenzo A., Arnal M., Albuerne J., Muller A. DSC isothermal polymer crystallization kinetics measurements and the use of the Avrami equation to fit the data: guidelines to avoid common problems Polymer Testing 26 (2007) 222-231
[48] Dell'Erba R., Groeninckx G., Maglio G., Malinconico M., Migliozzi A. Immiscible polymer blends of semicrystalline biocompatible components Thermal properties and phase morphology analysis of PLLA/PCL blends Polymer 42 (2001) 7831-7840
[49] A. T. Lorenzo, "Avrami and LH Plugin for Origin". Available at: https://sites.google.com/a/usb.ve/ajmuller/downloads/plugins June 2013
[50] Muller A., Avila M., Salazar J. Crystallization of PLA-based materials Science and Technology : Processing, Properties, Additives and Applications (2014) 66-98.
[51] Marand H., Xu J., Srinivas S. Determination of the Equilibrium Melting Temperature of Polymer Crystals Linear and Nonlinear Hoffman - Weeks Extrapolation Macromolecules 31 (1998) 8219-8229.